

***CARBOTHERMAL SYNTHESIS OF ALUMINUM NITRIDE
USING SUCROSE***

Youngmin Baik

**Department of Mining and Metallurgical Engineering
McGill University
Montreal, Canada**

December 1991

**A Thesis submitted to the Faculty of
Graduate Studies and Research
in partial fulfillment of the
requirement for the degree of
Master of Engineering**

© Y. Baik, 1991

*To my wonderful parents
&
my lovely fiancé Youngme.....*

ABSTRACT

In this work, the carbothermal reduction of Al_2O_3 to AlN was studied. Several kinds of aluminum oxides including $\alpha\text{-Al}_2\text{O}_3$, $\gamma\text{-Al}_2\text{O}_3$, $\theta\text{-Al}_2\text{O}_3$ and boehmite (AlOOH) were examined in order to observe the differences in reaction behaviour and powder characteristics obtained from each type of precursor. Cane sugar (sucrose) and carbon black were used as carbon sources. Reaction conditions studied were carbon to alumina ratio, temperature and reaction time. Sucrose resulted in a close-to-stoichiometric ratio of $\text{Al}_2\text{O}_3 : \text{C}$ (1 : 3.2) achieving full conversion to AlN and produced a regular powder morphology, whilst carbon black required higher ratio (> 1 : 4) to reach full conversion with agglomeration of the AlN powder. The optimal reaction temperature was 1600°C with the reaction time being dependent on the Al_2O_3 source. The results of the thermodynamic study for the Al-N-O-C system suggest a solid-state reaction process which is consistent with the experimental observations. Moreover, flowing N_2 gas flushes out the product CO gas and thus forces the equilibrium in favour of AlN formation. Reaction mechanisms are proposed for the two forms of carbon precursor.

RESUMÉ

Cette étude traite de la réduction carbothermique de l'oxide d'aluminium en nitrure d'aluminium. Plusieurs sortes d'oxide d'aluminium, comme α - Al_2O_3 , γ - Al_2O_3 , θ - Al_2O_3 et la bohémite (AlOOH) ont été utilisées dans le but d'observer les différents comportements au cours de la réaction, ainsi que les caractéristiques de la poudre obtenue pour chaque type de précurseurs. Le sucre de canne (sucrose) et le noir de carbone ont été utilisés comme source de carbone. Plusieurs conditions de réaction comme le rapport molaire entre le carbone et l'oxide d'aluminium, la température et le temps de réaction ont été étudiées.

L'utilisation de la sucrose en proportion stoechiométrique avec l'oxide d'aluminium (1 : 3.2) a permis une complète conversion en AlN et la production d'une poudre de morphologie régulière. Par contre, une proportion supérieure de noir de carbone ($> 1 : 4$) a été nécessaire pour atteindre une complète conversion, entraînant par ailleurs une agglomération de la poudre d' AlN . La température de réaction était optimale à $1600\text{ }^\circ\text{C}$, le temps de réaction étant dépendant de la source d' Al_2O_3 . Les résultats d'une étude thermodynamique pour le système Al-N-O-C suggère un processus de réaction à l'état solide, ce qui correspond aux observations expérimentales. De plus, l'utilisation d'un flux de N_2 permet d'éjecter le gaz CO produit lors de la réaction et ainsi de favoriser l'équilibre permettant la formation d' AlN . Des mécanismes de réaction sont proposés pour les deux précurseurs de carbone.

ACKNOWLEDGEMENTS

I would like to express my sincere gratitude to Prof. R.A.L. Drew for his supervision and encouragement throughout the course of this thesis.

I would like to thank Dr. K. Shanker for his suggestions and advice, as well as for his reviewing of the thesis.

I would also like to thank Mr. J.R. McDermid for his advice on the thermodynamic study, and also for his reviewing of the thesis.

Also I would like to thank Mr. D. Muscat for helping proof-read the thesis. Further thanks goes to Prof. M.D. Pugh for his suggestions and help during the course of this research.

I would also like to thank Miss L. Gavoret for translating the abstract into French and her encouragement to complete this thesis.

Special thanks goes to Mr. M. Knoepfel and all the machine shop personnel for their kind help in the workshop.

I would also like to thank all my colleagues in the ceramics group for their contribution to this work.

Finally, I would like to thank Ceralox Corporation for providing of several types of Al_2O_3 materials.

TABLE OF CONTENTS

ABSTRACT	ii
RESUMÉ	iii
ACKNOWLEDGEMENTS	iv
LIST OF FIGURES	viii
LIST OF TABLES	x
CHAPTER 1. INTRODUCTION	1
CHAPTER 2. LITERATURE REVIEW	3
2.1 Properties of Aluminum Nitride	3
2.1.1 Thermal and Electrical Properties of Aluminum Nitride	3
2.1.2 Chemical and Physical Properties of Aluminum Nitride	5
2.2 Aluminum Nitride Powder Synthesis	6
2.2.1 Direct Nitridation to Aluminum Nitride	7
2.2.2 Carbothermal Reduction to Aluminum Nitride	8
2.2.3 Other Methods of Aluminum Nitride Synthesis	13
2.3 Sintering Behaviour of Aluminum Nitride	13
CHAPTER 3. OBJECTIVES	16
CHAPTER 4. EXPERIMENTAL PROCEDURE	17
4.1 Starting Materials	17
4.2 Precursor Mixing	17
4.3 Precursor Pyrolysis	19

4.4 Carbothermal Reduction	20
4.5 Decarburization	22
4.6 Sintering	24
4.7 Analysis	25
4.7.1 X-Ray Diffraction	25
4.7.2 Particle Size Analysis	26
4.7.3 Specific Surface Area	27
4.7.4 Scanning Electron Microscopy	27
4.7.5 Chemical Analysis	28
4.7.6 Thermal Conductivity Measurement	28
4.8 Thermodynamic Modelling of the Al-N-O-C System	29
4.8.1 Objectives of the Modelling	29
4.8.2 Modelling Method	30
CHAPTER 5. RESULTS AND DISCUSSION	32
5.1 Effect of Al ₂ O ₃ : C Ratios on Conversion	32
5.2 Effect of Reaction Temperature on Conversion	35
5.3 Thermodynamic Modelling of Al-N-O-C System	42
5.4 Effect of Reaction Time on Conversion	49
5.5 Relationship between the Particle/Agglomerate Sizes of the Precursor Al ₂ O ₃ and AlN Product with Reaction Time	52
5.6 Reaction Mechanism and Nitridation	63
5.6.1 Effect of Carbon Source	63

5.6.2 Mechanism of Nitridation	66
5.7 Sintering and Thermal Conductivity	69
CHAPTER 6. CONCLUSIONS AND FUTURE WORK	72
6.1 Conclusions	72
6.2 Suggested Future Work	75
REFERENCES	76
APPENDICES	80
APPENDIX 1. QUANTITATIVE X-RAY DIFFRACTION ANALYSIS	81
APPENDIX 2. THERMODYNAMIC DATA OF THE Al-N-O-C SYSTEM	83
APPENDIX 3. CALCULATION FOR A RATIO OF $Al_2O_3 : C$	98

LIST OF FIGURES

Figure 2.1:	General carbothermal reduction process.	9
Figure 2.2:	TGA of the decarburization process.	11
Figure 4.1:	Schematic diagram of the reactor for carbothermal reduction.	21
Figure 4.2:	Schematic diagram of the decarburization of AlN.	23
Figure 5.1:	AlN conversion vs. Al ₂ O ₃ :C ratio at 1600 °C for 5 hours.	33
Figure 5.2:	AlN conversion rate vs. reaction temperature (reaction time of 5 hours) using Bacosol 3C and A16SG and cane sugar as a carbon source. (Al ₂ O ₃ : C = 1 : 3.5).	36
Figure 5.3:	The Arrhenius plot of ln conversion rate vs. 1/T for Bacosol 3C and A16SG.	38
Figure 5.4:	Micrograph of AlN powder nitrided from Bacosol 3C at 1550 °C, (a) mixture of AlN and Al ₂ O ₃ , (b) unreacted Al ₂ O ₃ , (c) EDS analysis of (b) showing O ₂ peak, (d) fully converted AlN at 1600 °C and (e) fully converted AlN at 1650 °C.	40, 41
Figure 5.5:	Partial pressure of (a) N ₂ and CO, (b) O ₂ vs. amount of N ₂ gas introduced at 1600 °C. (Al ₂ O ₃ : C = 1 : 6)	45
Figure 5.6:	Partial pressure of O ₂ as a function of reaction temperature.	46
Figure 5.7:	Combined predominance diagrams of Al-N-O-C system (a) at 1450 °C, 1500 °C and 1550 °C, (b) 1600 °C, 1650 °C and 1700 °C. P(O ₂) vs. P(CO), P(N ₂) is constant (0.972 atm).	48
Figure 5.8:	The conversion of Bacosol 3C, T40X, and HPA-0.5 as a function of reaction time at 1600 °C. (at 1500 °C for T40X)	51
Figure 5.9:	Variation in particle sizes of the AlN powders produced using (a) Bacosol 3C, (b) T40X, (c) HPA-0.5 with a different reaction time.	54,55
Figure 5.10:	Typical examples of particle size distribution graphs of AlN from (a) Bacosol 3C, (b) T40X, (c) HPA-0.5 provided by NICOMP particle size analyser.	56

Figure 5.11: Micrographs of AlN powders produced using (a) HPA-0.5, (b) A16 SG, (c) Bacosol 3C, (d) Pural 200, (e) T40X, (f) SOL-P3 with cane sugar as a carbon source at 1600 °C for five hours, and commercial powders (g) Tokuyama Soda, (h) Starck C.	59 - 62
Figure 5.12: Micrographs of AlN powders produced using A16SG and (a) cane sugar and (b) carbon black as a carbon source.	65
Figure 5.13: The schematic models of the anticipated reaction sequences when (a) cane sugar and (b) carbon black are used as a carbon source.	67,68
Figure I: XRD calibration curve for quantification of unreacted Al ₂ O ₃ in AlN powder.	82
Figure II.1: Partial pressure of CO ₂ vs. amount of N ₂ gas introduced at 1600 °C (Al ₂ O ₃ : C = 1 : 6).	85
Figure II.2: Partial pressure of Al ₂ O ₂ vs. amount of N ₂ introduced at 1600 °C (Al ₂ O ₃ : C = 1 : 6).	86
Figure II.3: Partial pressure of CO ₂ as a function of temperature	87
Figure II.4: Partial pressure of Al ₂ O ₂ as a function of temperature	88

LIST OF TABLES

Table 2.1:	Thermal and electrical properties of AlN and those of other substrate materials and of Si.	4
Table 2.2:	Physical properties of AlN, BeO, and Al ₂ O ₃ .	5
Table 4.1:	Physical and chemical analysis of Al ₂ O ₃ sources.	18
Table 5.1:	The Gibbs energy change for the possible reactions of carbothermal reduction of Al ₂ O ₃ to AlN.	43
Table 5.2:	Partial pressures of N ₂ , CO, CO ₂ , Al ₂ O ₂ and O ₂ for the equations of Al ₂ O ₃ + 3C + 106.5N ₂ and Al ₂ O ₃ + 6C + 106.5N ₂ at 1600 °C.	44
Table 5.3:	AlN powder characteristics produced from different precursors (1600 °C for 5 hours, Al ₂ O ₃ : C = 1 : 6)	58
Table 5.4:	The fired density, chemical analysis, and thermal conductivity values of sintered pellets.	71
Table II.1:	Partial pressures of N ₂ , CO, CO ₂ , Al ₂ O ₂ and O ₂ for the equation of Al ₂ O ₃ + 3C + <A>N ₂ at 1873 K.	83
Table II.2:	Partial pressures of N ₂ , CO, CO ₂ , Al ₂ O ₂ and O ₂ for the equation of Al ₂ O ₃ + 3C + 106.5N ₂ , at several temperatures	83
Table II.3:	Partial pressures of N ₂ , CO, CO ₂ , Al ₂ O ₂ and O ₂ for the equation of Al ₂ O ₃ + 6C + <A>N ₂ , at 1873 K.	84
Table II.4:	Partial pressures of N ₂ , CO, CO ₂ , Al ₂ O ₂ and O ₂ for the equation of Al ₂ O ₃ + 6C + 106.5N ₂ , at several temperatures.	84

CHAPTER 1: INTRODUCTION

One of the important applications of advanced ceramics is their use in integrated circuit substrate materials. Until recent years, most of the interest in the development of integrated circuits has concentrated on low-power, low-density circuits and, therefore, the thermal properties of substrate materials were not of great concern. Today, however, the rapid development of more complex circuits with larger chip sizes and great power consumption brings about the need for new materials which have high thermal conductivity, low thermal expansion, high electrical insulation, high dielectric breakdown strength, high mechanical strength, ease in cutting and polishing, high chemical stability and non-toxicity.¹

The properties of AlN satisfy most of properties stated above. The thermal conductivity of AlN is eight times as high as that of Al₂O₃ at room temperature, and is almost equal to that of 99.5 % BeO at 150 °C. The coefficient of thermal expansion of AlN is smaller than that of Al₂O₃ and BeO, and is close to that of the Si semiconductor.²

Currently, the most popular substrate material for integrated circuits is Al₂O₃. More than 90 % of substrates are made of Al₂O₃, the remainder being made from beryllia (BeO), silicon carbide (SiC), glass composites, and aluminum nitride (AlN). Even though BeO has higher thermal conductivity than AlN, the use of BeO is decreasing due to its toxic nature. According to the requirements for substrate material and the properties of AlN, Al₂O₃ and BeO described above, AlN seems to be one of the more promising materials for thermomechanical and high performance

electronic ceramic applications.

AlN can also be made translucent or transparent if it is of high purity and high density, which, when combined with its wear resistance, make AlN attractive for some electro-optics applications. AlN is also added to modify the thermal expansion of glasses or polymers used as substrate materials in some application, thereby minimize thermal mismatch problems.^{3, 4}

Besides the use of AlN in electronic applications, AlN has been used in structural applications, such as crucibles and refractories. Moreover, its unique properties; high thermal conductivity, high specific modulus and low thermal expansion make it potentially useful for both monolithic and composite AlN parts in heat-engine applications. AlN powder compacts can be infiltrated with molten aluminum to produce fully dense bodies having excellent strength and stability. Other potential structural applications are for refractories in nitrogen and hydrogen furnaces, seals and rings, grinding media, and contact parts for chemical processes; this is mainly due to its high melting temperature and resistance to chemical attack.⁵

This thesis deals with AlN synthesis by carbothermal reduction or nitridation of aluminum oxides. The objectives are to establish the important processing conditions and the factors affecting the conversion of Al_2O_3 to AlN and the thermal conductivity of final AlN powder.

CHAPTER 2: LITERATURE REVIEW

2.1 PROPERTIES OF ALUMINUM NITRIDE

2.1.1 Thermal and Electrical Properties of Aluminum Nitride

Aluminum nitride has attractive thermal and electrical properties for high density and high power integrated circuit applications. Table 2.1⁶ shows its thermal and electrical properties along with those of other ceramic materials which are currently used in the above applications. Also included in Table 2.1 are the thermal and electrical properties of Si, which is the main semiconductor material used in integrated circuits. The thermal conductivity of single crystal AlN is estimated to be 320 W/m·K but that of sintered polycrystalline AlN is generally found to be about 80 - 200 W/m·K.^{1 - 4} Its coefficient of thermal expansion (CTE) is $4.4 \times 10^{-6}/^{\circ}\text{C}$, which is very close to that of silicon ($3.2 \times 10^{-6}/^{\circ}\text{C}$).² These two properties make it possible that AlN can be used in high power, high density circuits as substrate materials rather than other ceramic materials which exhibit lower thermal conductivities and/or higher CTEs. Because in high power, high density circuits, large amounts of heat are produced during operation, if a substrate material does not have high thermal conductivity and CTE to that of the Si chips, either the substrates or Si chips may fail during operation. In addition, AlN's electrical properties, such as its electrical resistivity ($10^{14}\Omega\cdot\text{cm}$), dielectric constant (8.9), and breakdown voltage (15 kV/mm) are equally as good as the other ceramic materials used for this type of application.

Slack et al.⁹ measured the thermal conductivity of high purity, single crystal

AlN over a wide temperature range and obtained a value of 319 W/mK at 300 K. One reason for the decrease in thermal conductivity of AlN ceramics is oxygen. It has been reported by Kuramoto⁶ that the thermal conductivity of AlN is drastically affected by oxygen and other metallic impurities such as Si, Fe and Mg. When oxygen substitutes for nitrogen in the AlN lattice, it creates aluminum vacancies due to the difference in valency between oxygen and nitrogen. This creation of vacancies leads to phonon scattering and thereby lowers the thermal conductivity far below that of pure AlN single crystals (320 W/m·K).^{7, 8} Furthermore, if there are any other metallic impurities (e.g. Mg, Si, Be)^{6 - 8} in the AlN lattice, phonon impurity interactions occur and cause the thermal conductivity to be reduced still further. Therefore, to obtain high thermal conductivity AlN, it is very important to produce powder which contains extremely low amounts of oxygen and metallic impurities.

Table 2.1 Thermal and electrical properties of AlN and, those of other substrate materials and of Si⁶

	AlN	Al ₂ O ₃	BeO	Si
Thermal conductivity (W/m·K) at room temperature	160 (320)*	20	260 (370)*	120
C.T.E (x 10 ⁻⁶ /°C) room temperature - 400 °C	4.4	7.2	8.0	3.2
Volume resistivity (Ω·cm)	10 ¹⁴	10 ¹⁴	10 ¹⁴	10 ⁻³ -10 ³
Dielectric constant, 1 MHz	8.9	9.4	7.0	12.0
Dielectric loss (x 10 ⁻⁴), 1 MHz	8	4	3	
Dielectric strength (kV/mm)	15	15	10	10

*:theoretical value

2.1.2 Chemical and Physical Properties of Aluminum Nitride

Pure aluminum nitride is a III-V insulating compound which crystallizes with the wurtzite structure. There are no other known polytypes. The theoretical density is 3.25 g/cm^3 and it is colourless and optically transparent when pure.⁹ The melting point or decomposition point of AlN has been reported to be $2800 \text{ }^\circ\text{C}$ under 100 atm. pressure of N_2 ⁹. Elsewhere¹⁰, it was reported that at atmospheric pressure, AlN decomposes into aluminum and nitrogen at $2450 \text{ }^\circ\text{C}$.

Some physical properties of AlN, along with those of BeO and Al_2O_3 , are tabulated in Table 2.2.^{2, 11} The flexure strength of AlN at room temperature (35 - 50 MPa) is much higher for Al_2O_3 (31 - 32 MPa) and BeO (25 MPa). On the other hand, the Vickers hardness of AlN (1200 MPa) is half of that of Al_2O_3 (2300 - 2700 MPa). These factors mean that AlN is stronger than Al_2O_3 and BeO but more easily machinable than Al_2O_3 .

Table 2.2 Physical properties of AlN, BeO, and Al_2O_3 ^{2, 11}

	AlN	BeO	Al_2O_3
Purity (%)	>99.5	99.5	>99
Density (mg/cm^3)	3250	2900	3890
Vickers hardness (kg/mm^2)	1200	1200	2300-2700
Flexure strength (MPa)	340-490	245	304-314
Light transmission (%) ($\lambda = 6 \mu\text{m}$, $t = 0.5 \text{ mm}$)	48	opaque	opaque

However, AlN has also a disadvantage in that it is very easily oxidized in air

and in the presence of moisture. The oxidation of AlN proceeds by several mechanisms:¹

(1) low-temperature hydrolysis (around 100 °C)



(2) high-temperature hydrolysis (100 - 300 °C)



(3) high temperature oxidation. (300 - 700 °C)



Each one of these reactions can occur during the burn off of excess carbon from processing of AlN, in air or during the storage of the powder in wet conditions. The typical surface oxidation rate of AlN was reported by Slack et al.⁹ to be 50 to 100 Å of oxide per day at room temperature.

As stated in the previous section, oxygen in the AlN lattice lowers its thermal conductivity. Hence, AlN powder should not be too fine; otherwise surface oxidation reaches excessively high levels. However, since good sinterability and high thermal conductivity requires fine powder (and grain size), the optimum particle size is believed to be ~0.1 - 1 µm.¹²

2.2 ALUMINUM NITRIDE POWDER SYNTHESIS

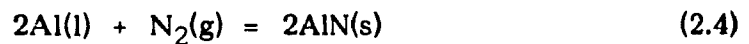
Aluminum nitride can be synthesized using a variety of processing methods. For producing commercial AlN powder, the direct nitridation of Al and the carbothermal reduction of Al₂O₃ are used. There are several other methods to

produce AlN powder, such as the chemical vapour deposition (CVD) method, polymer pyrolysis and arc plasma method.³

In this section, the carbothermal reduction process will be described and discussed. Direct nitridation and other methods will also be described, but in much less detail.

2.2.1 Direct Nitridation of Aluminum to Aluminum Nitride

Direct nitridation of Al occurs by the reaction of Al metal powder with nitrogen and proceeds rapidly above 1200 °C according to the following equation:³



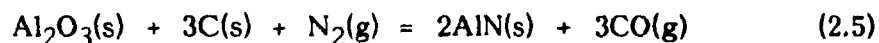
Since metallic Al (which agglomerates very easily) is used as a starting material, it naturally requires a pulverizing step to decrease the particle size and increase the rate of nitridation. Furthermore, in order to increase the sinterability of the nitrated powder, it requires a final milling step to reduce the particle size of the resulting hard agglomerates to less than several microns. The advantages of this process are that the reaction is simple and the cost of the operation and of raw materials are cheap. However, the pulverizing steps are usually carried out using a ball mill, and therefore, it is impossible to avoid contamination by metals or metallic compounds from the mill.⁵ Furthermore, it is extremely difficult to produce AlN powder without unreacted metallic Al as an impurity. Since direct nitridation to AlN takes place at a temperature above the melting point of Al (660°C), if the temperature is raised too fast or too high, pulverized metallic Al can

melt and agglomerate prior to nitridation, thus remaining unreacted Al as in the nitrided powder. It is hard to reduce the amount of impurities from the two milling steps as well as the unreacted metallic Al to less than several weight %. Acid washing is frequently required to remove metallic contamination. Surface oxidation of the AlN powder also occurs during milling. Therefore, AlN powder produced by direct nitridation method usually contains at least 2 - 5 weight % oxygen.⁵

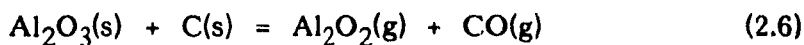
2.2.2 Carbothermal Reduction of Alumina to Aluminum Nitride

Carbothermal reduction of Al₂O₃ to AlN involves intimate mixing of various forms of aluminum oxide with a source of carbon, and must take place at high temperature³ in a flowing nitrogen atmosphere or under high pressure. The carbothermal reduction process is schematically shown in Figure 2.1.

The overall reaction of carbothermal reduction is as follows¹:



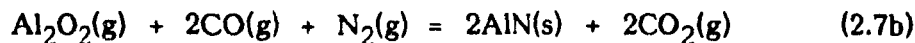
This reaction takes place at a temperature of 1400 °C to 1700 °C. Shanker et al. have suggested that this reaction may proceed via two steps:¹⁴



and



and/or



The thermodynamic study on these reactions will be discussed in Chapter 5.

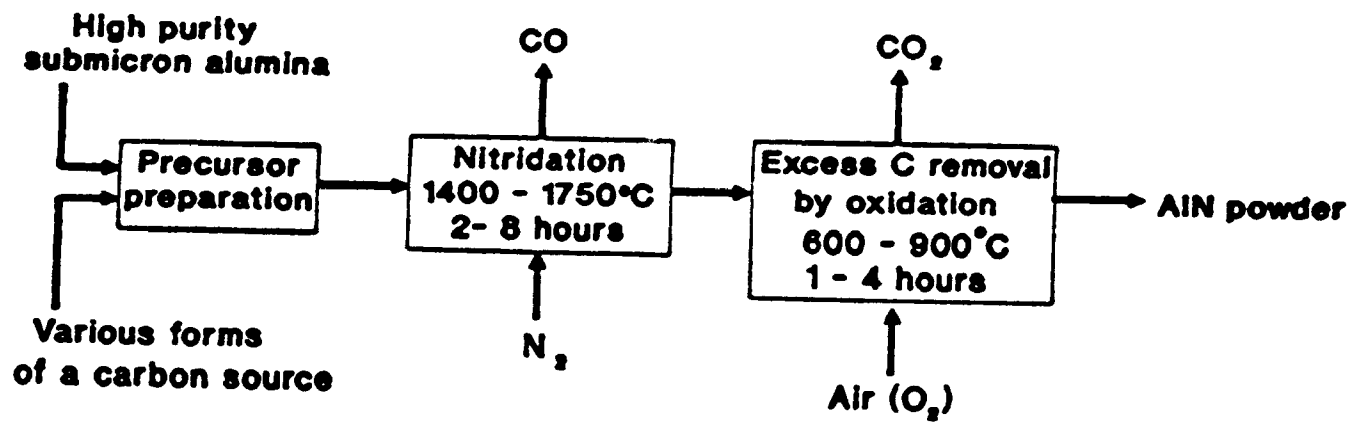


Figure 2.1 General carbothermal reduction process

In reaction 2.5 carbon reduces Al_2O_3 , which then reacts with nitrogen to form AlN. Although the stoichiometric ratio of $\text{Al}_2\text{O}_3 : \text{C}$ is 1 : 3, higher ratios ($\text{Al}_2\text{O}_3 : \text{C} = 1 : 3.4 - 34$) were necessary to realize full conversion to AlN in most of recent studies.^{5, 15, 16} It is thought that the need for excess C arises from the fact that, even when the C source is mixed well with Al_2O_3 , each particle of Al_2O_3 can not be coated with a stoichiometric ratio amount of C. Therefore, to contact stoichiometric amounts of C with Al_2O_3 particles to get full conversion to AlN, it is necessary to use an excess of carbon. The amount of excess carbon will depend on the choice of raw materials and the mixing procedure, as will be discussed in Chapter 5. Because of the use of excess of carbon, it is necessary to burn off the residual carbon at a temperature of 600 °C to 900 °C in dry air after carbothermal reduction.⁵ A study using thermogravimetric analysis (TGA) to analyze the decarburization process, shown in Figure 2.2¹⁷, suggests oxidation of the carbon begins near 600 °C. The weight loss curve has two distinct slopes, the first slope starts near 600 °C and the second slope starts just below 700 °C and ends at 800 °C, suggesting that some of the carbon is strongly bonded with the AlN and is more difficult to remove. The weight gain near 1100 °C is due to oxidation of AlN according to reaction 2.3. After following this processing method, Kuramoto et al.⁵ obtained fine AlN powder which has an average particle diameter of not more than 2 μm and contained at least 94 wt% of AlN, less than 3 wt% of O_2 and less than 0.5 wt% of metal impurities.

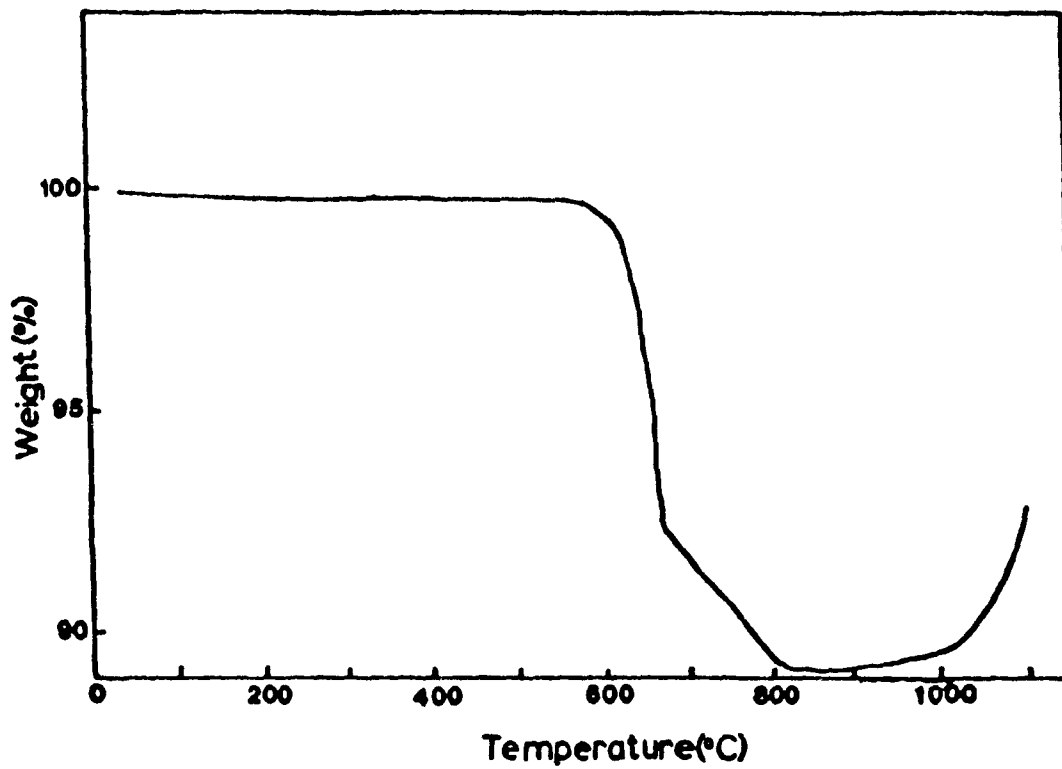


Figure 2.2 TGA (thermogravimetric analysis) on the decarburization process.¹⁷

Other investigators have succeeded in producing high purity AlN powder using carbothermal reduction: Lee et al.¹⁸ found that nitridation at 1500 °C for 8 hours resulted in conversion to 97 % AlN with 3.1 wt% oxygen and 2.5 wt% carbon. Commercial manufacturers such as Sumitomo Chemical produces AlN powders containing > 98 wt% AlN with < 1.6 wt% oxygen and < 0.2 wt% carbon, with particle sizes < 3 μm. Dow Chemical also produce AlN powder by carbothermal reduction with an average particle size of 1.5 μm containing 1.2 wt% oxygen and 0.13 wt% carbon.¹⁹

It is important to keep the amount of excess carbon to a minimum in order to avoid any residue in the AlN after the decarburization step. The choice of carbon can help reduce this. There are several candidate materials which can be used as a carbon source. In most of studies to date, carbon black with high surface area, typically ~160 m²/g, is employed with Al₂O₃ : C ratios of 1 : 3.4 up to 1 : 34.^{5, 14, 16} Furfuryl alcohol (2-(C₄H₃O)CH₂OH)) has also been used as a carbon source. Furfuryl alcohol is mixed with hydrated alumina and then carburized at low temperature (~100 °C) for three days.^{17, 18}

To produce high purity, sub-micron particle size AlN, it is necessary to use sub-micron particle size aluminum oxide containing low metallic impurities. The raw material selected is usually α-Al₂O₃. However, other hydrated compounds, such as boehmite (AlO·OH), aluminum trihydrate (Al(OH))₃¹⁵ or aluminum isopropoxide (Al[OCH(CH₃)₂])₃^{18, 20} have been used. No significant effect of using the different forms of alumina on the reaction to AlN has been reported.¹⁵

2.2.3 Other Methods of Aluminum Nitride Synthesis

There are several other methods used to produce AlN. Two examples are based on chemical vapour deposition (CVD) and polymer pyrolysis. In the former, AlN powder is synthesized by the vapour-phase reaction of AlCl_3 and NH_3 at 600 - 1100 °C, which then deposits on the wall of the reactor. The purity of AlN produced by this method is very high since the reactants themselves can be prepurified by distillation and by sublimation. However, this process is limited to laboratory scale because a large amount of HCl byproduct is evolved.^{3, 13}

Aluminum Nitride can also be produced by an arc plasma method. Aluminum powder reacts with NH_3 in a triple d.c. torch plasma reactor or in a parallel plate plasma reactor, and forms single crystal AlN powder. The power used for operating a plasma torch is 0.5 - 30 kW depending on the through-put required.^{3, 13}

High purity, very fine (< 0.01 μm) AlN powder can be produced by the above methods, however, the disadvantages of these processes are that the very fine AlN powder is easily oxidized in air (see above) and the manufacturing cost is much higher than for the carbothermal reduction or direct nitridation process. Therefore, these methods are still at a laboratory scale and are undergoing further research.

2.3 SINTERING BEHAVIOUR OF ALUMINUM NITRIDE

There are three ways to sinter AlN: pressureless sintering, hot pressing, and hot isostatic pressing (HIP). The sintering of AlN is typically carried out in the temperature range of 1600 °C - 2100 °C.⁵ It was reported that the average particle

diameter of AlN powder should not exceed 2 μm in order to achieve a high density and high thermal conductivity AlN ceramic. Furthermore, the oxygen content should be less than 1.5 wt % and its metallic impurities less than 0.1 wt %.⁵

It has been reported by Virkar et al.⁷ that thermal conductivity increases with the amount of additive and post sintering annealing time. Annealing was performed after sintering at 1850 °C for between 1 and 1000 minutes and 1 - 4 wt% of either Y_2O_3 , Dy_2O_3 , or Yb_2O_3 was used as an additive, annealed for 6 hours at 1810 °C to ensure uniform treatment of the samples. Thermal conductivity was also found to depend on the type of sintering additive used. It has been generally recognized that rare-earth or alkaline-earth oxide additives react with Al_2O_3 to form aluminates and effectively purify the AlN lattice by removing dissolved oxygen and thus enhance the phonon mean free path.⁷ Buhr et al.²¹ also explained that the liquid phases formed by oxide additives at the sintering temperature eliminated at least part of the Al_2O_3 content from the AlN lattice, thus improving the thermal conductivity. Virkar et al.⁷ used 2 wt% Y_2O_3 , Dy_2O_3 , CaO and Yb_2O_3 as sintering additives to Tokuyama Soda AlN. The sample containing Dy_2O_3 resulted in a thermal conductivity of 160 W/m·K, whilst the samples containing Yb_2O_3 and CaO had values of 147 W/m·K and 137 W/m·K, respectively. Other workers^{22,23} have reported that Eu_2O_3 , CeO, La_2O_3 , and SiO_2 can be used as sintering aids. It was also suggested that the use 3 - 5 wt% of oxide sintering aids can maximize the thermal conductivity of AlN.²¹ Because the thermal conductivity of aluminates are lower than that of AlN, there is an optimum amount of the second phase corresponding to

a maximum in the thermal conductivity. Initially, the thermal conductivity increases with an increasing amount of the additive because of improved purification of the AlN lattice. Once a sufficient amount of the additive is available for forming aluminates, further additions of the sintering aid decrease the thermal conductivity.⁷

In the sintering of AlN ceramics, the processing conditions, such as sintering temperature, the type and amount of sintering additive, the role of pressure (for HIP or hot pressing), etc. are not well understood and optimum sintering conditions have yet to be established.

CHAPTER 3: OBJECTIVES

The aims of this study are:

- 1) To produce high purity, sub-micron particle size AlN powder using the carbothermal reduction process.

- 2) To study the use of cane sugar as a source of carbon and to determine the carburization conditions as well as to establish the possible advantages of the use of cane sugar in terms of powder reaction kinetics and product quality.

- 3) To establish the effect of alumina source on the AlN powder produced.

- 4) To understand the effect of reaction time and temperature on the degree of conversion of Al_2O_3 to AlN, and their influence on the morphology of the AlN powder produced.

- 5) To understand the mechanism of the carbothermal nitridation reaction with respect to cane sugar and carbon black as precursor materials

CHAPTER 4: EXPERIMENTAL PROCEDURE

4.1 STARTING MATERIALS

In this study, experiments were carried out using two sources of carbon: carbon black and cane sugar, and seven different aluminas/boehmites, as listed in Table 4.1.

The carbon black (Monarch 1300), provided by Cabot Corporation, had relatively high levels of cyanide (~6.33 ppm) and phenols with significant trace amounts of nickel (16.4 ppm), chromium (~11.8 ppm) and iron (< 10 ppm). Cane sugar which was bought at a grocery store, was predominantly sucrose (C₁₂H₂₂O₁₁) the main impurity being Fe (5 ppm). The aluminas, since they are produced by the Bayer process, contained the usual SiO₂, Na₂O and Fe₂O₃ impurities as shown in Table 4.1.

4.2 PRECURSOR MIXING

The starting materials were combined by three separate wet mixing methods viz. attrition milling, impeller mixing, and ball milling.

Attrition milling was carried out in a plastic container of 4 L capacity. The mixture of raw materials and alumina media (3.75 mm diameter, 99.7% purity) were milled in distilled water for 30 minutes at 200 rpm. The ratios of raw material to media and raw material to water were 1:3 by weight. Impeller mixing was carried out in a glass beaker (500 mL) and this method was used only for hydrated aluminas (Bacosol 3C and Bacosol 3A which contain 60 - 70 % water). The hydrated aluminas

Table 4.1 Physical and chemical analysis of Al₂O₃ sources.
(suppliers data)

Al ₂ O ₃ SOURCE	TYPE OF Al ₂ O ₃ SOURCE	SURFACE AREA (m ² /g)	PARTICLE SIZE (μm)	Chemical Analysis SiO ₂ , Fe ₂ O ₃ , Na ₂ O (ppm)
A16SG*	α-Al ₂ O ₃	9	0.3-0.5	250, 100, 800
Bacosol 3C●	AlOOH (boehmite) ⁺	150-200	0.1-0.2	70 (SiO ₂)
Bacosol 3A●	AlOOH (boehmite) ⁺	150-200	0.1-0.2	70 (SiO ₂)
T40X [○]	θ-Al ₂ O ₃	39.4	0.07	186.4, 334.2, 16.3
HPA-0.5 [○]	α-Al ₂ O ₃	9.1	0.3	51.4, 57.1, 94
Alumina Sol P-3 [○]	γ-Al ₂ O ₃	316	0.02	N/A
Pural 200 [○]	AlOOH (boehmite)	85	0.038	N/A

N/A: not available

+: in the form of sol (60 - 70 % water containing)

Suppliers: *Alcoa
● Alcan
○ Ceralox

(in the form of a boehmite sol) were mixed with sugar for 30 minutes without any additional water. Ball milling was carried out in a 1L plastic jar for most experiments. Raw materials were mixed with Al_2O_3 ball media (6.5 mm diameter, 99.7 % purity) for 18 hours. The ratio of raw material to media was 1:5 by weight.

All mixtures of Al_2O_3 and carbon black were then microwave dried to rapidly remove the majority of the water, followed by complete drying in an oven at 120 °C for 18 hours and then at 300 °C for 5 hours. In those cases where cane sugar was the carbon source, all the precursors were directly pyrolyzed after mixing.

4.3 PRECURSOR PYROLYSIS

The precursors that contained sugar needed to be pyrolyzed in order to convert the sugar to carbon. Pyrolysis was carried out in a furnace by following a sequence of temperature increments steps. To remove the large amount of water used as a solvent (~65 %), it was necessary to maintain the precursors at 120 °C for 18 hours. After water removal, the precursor pyrolysis was as follows: 140 °C for 4 hours, 170 °C for 18 hours, 210 °C for 18 hours, and 235 °C for 18 hours. After following these steps, the yield of carbon was determined to be 20 - 25 wt. % of the starting sucrose ($\text{C}_{12}\text{H}_{22}\text{O}_{11}$). The calculated theoretical yield of carbon from sucrose ($\text{C}_{12}\text{H}_{22}\text{O}_{11}$), assuming only water removal, is 42.11 wt.%. It was necessary to maintain careful control over the pyrolysis since the carburization of sucrose is exothermic, which may lead to the temperature exceeding tolerable ranges, thus reducing the carbon yield.

After pyrolysis, the precursor was quite hard but porous, while the precursor from carbon black was soft and relatively dense. The approximate bulk density of the precursor using cane sugar as a carbon source was 0.3 g/cm^3 and that using carbon black was 0.5 g/cm^3 . The precursor materials were broken down, by hand, into $1 - 3 \text{ cm}^3$ size irregular shaped lumps prior to nitridation.

4.4 CARBOTHERMAL REDUCTION

All carbothermal reduction experiments were carried out in a horizontal, controlled atmosphere, graphite element resistance furnace. The thermocouple used for this furnace was the type C (W-5% Re vs. W-26% Re) provide by the Omega Engineering Inc.. The reactor, as shown schematically in Figure 4.1, was made of high density graphite (Speer Canada, grade 3499), with an inside diameter of 14 cm and a height of 16 cm. The base of the reactor consisted of a graphite plate used to support the reactants. This graphite plate had an arrangement of 3 mm holes which allowed the N_2 gas to flow over the reactants. To prevent the reactants from falling through the holes, a thin graphite felt was placed on the graphite plate. In some experiments, the inside of the reactor was divided into four segments to allow for reaction of up to four precursor materials under the same conditions. When one batch of precursor material was nitrided, a minimum of 20 g and a maximum of 200 g of material was loaded in the reactor. When the reactor was divided into four segments, about 20 - 50 g of material was loaded in each segment.

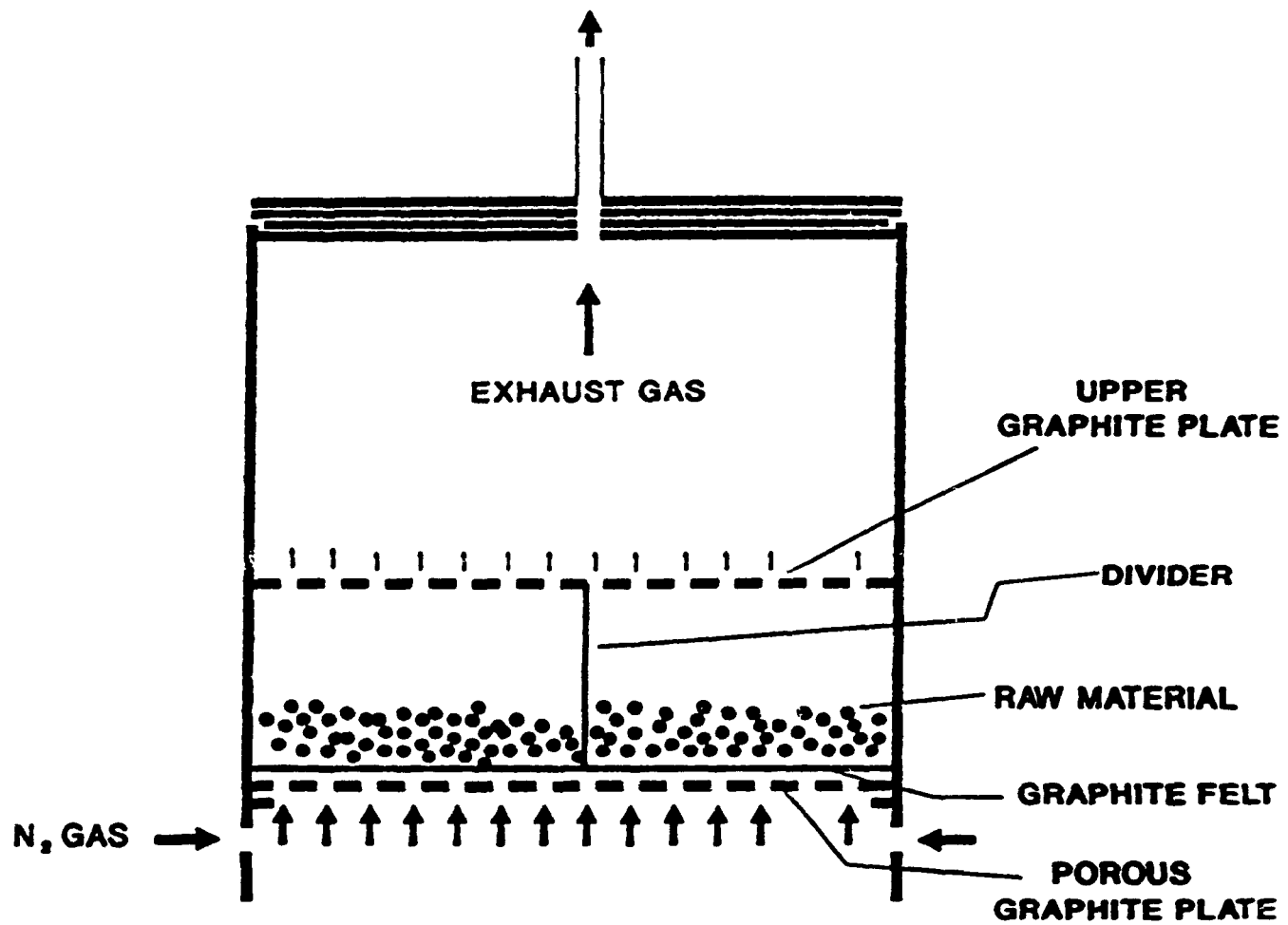


Figure 4.1 Schematic diagram of the reactor for carbothermal reduction.

Pre-purified grade (Linde Union Carbide), preheated nitrogen gas (contained $O_2 \leq 3$ ppm, $H_2O \leq 5$ ppm) was introduced from the bottom of the reactor, at a linear flow rate of 0.2 cm/sec. Before introducing the N_2 gas, the furnace was evacuated to less than 0.004 kPa in order to eliminate air and water vapour from the system. The furnace was heated up to 200 °C in manual mode for 30 minutes and then turned into automatic mode to increase temperature up to the set reaction temperature (1500 - 1650 °C) for one hour. After the temperature reached set point, it was maintained for the reaction time, which was mostly five hours, except in the case of the reaction time study experiments, and was then furnace was turned off and cooled down. The exhaust gas was passed through a gas bubbler, filled with 3 % diluted sodium hypochlorite to capture potential cyanide gas, which may have been produced from reactions between carbon²⁴ and nitrogen.

4.5 DECARBURIZATION

After nitridation, some amount of excess carbon still remained. The simplest method to remove this unreacted carbon is to burn it off in air.

The decarburization cycle consisted of a small amounts of product (~5 g) of the as-reacted materials being placed in alumina crucibles, 5 cm in diameter and 1 cm high, and heating in an electrical resistance furnace at a temperature of 750 °C for a time of 2 to 24 hours. For larger batches, decarburization was carried out in a flowing air decarburizer, illustrated in Figure 4.2, operating at a temperature of ~730 °C for 5 to 6 hours. The decarburizer was made of a mullite tube and a porous

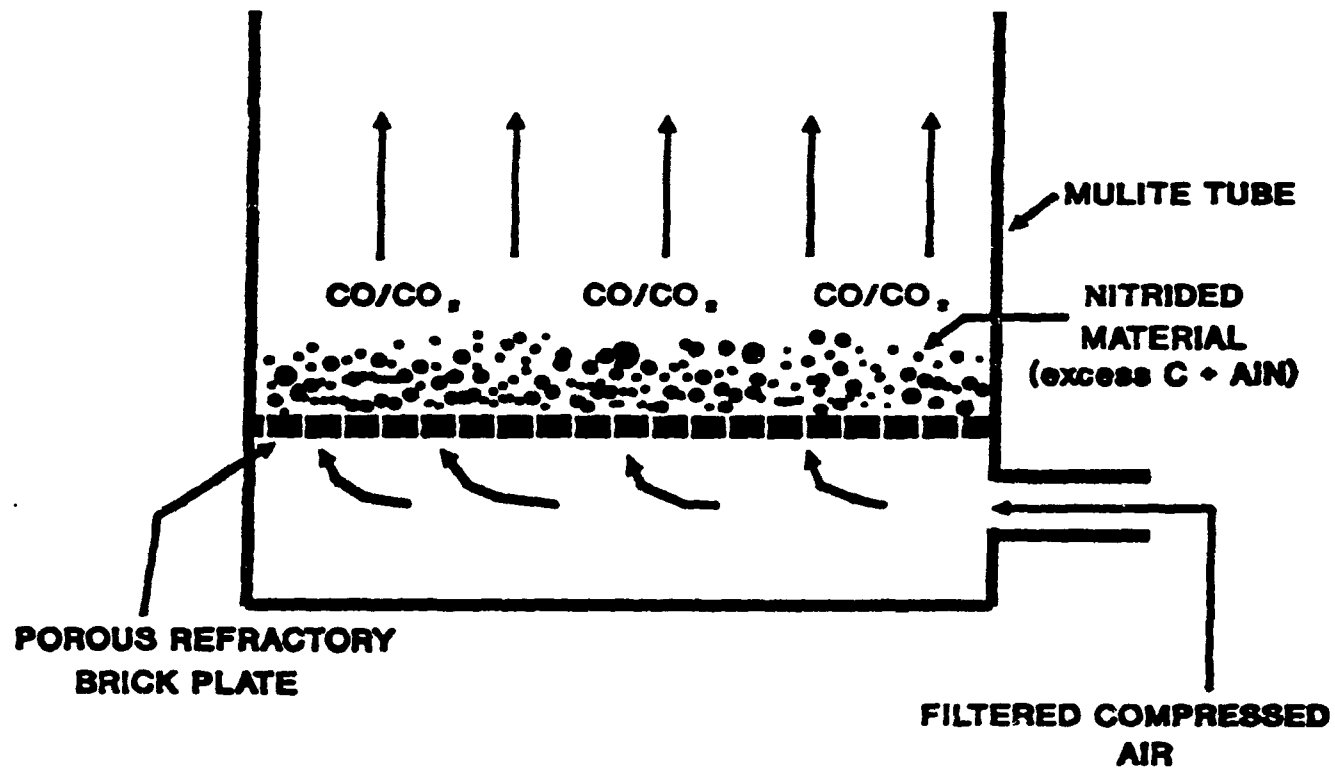


Figure 4.2 Schematic diagram of the AlN decarburization.

refractory brick plate. As seen in Figure 4.2, the synthesized materials sat on the refractory brick plate, and air was introduced into the space below the plate and passed through the plate to remove the CO and CO₂ gases produced in the reactor. Compressed air was used and passed through a filter to remove oil and other contaminations before introducing it into the decarburizer at a flow rate of ~10 L/min.

In cases where $C : Al_2O_3 \geq 10$, there was enough excess carbon to cause the temperature to rise exothermally. As a result, not only the carbon was oxidized but also the AlN during decarburization. In this case, the temperature had to be raised slowly and kept at 650 °C for 5 hours and then increased to 730 °C for 5 to 6 hours.

4.6 SINTERING

Aluminum nitride powders were attrition milled with 4 wt.% Y₂O₃ (Union Molycorp, 5603X) in reagent grade isopropanol at 200 rpm with high purity (99.5 %) Al₂O₃ media for 30 minutes. The volume of isopropanol and the weight of media used were both five times the powder weight. After milling, the powders were dried in a microwave oven until semi-dry, and then fully dried in an oven. Dried powders were granulated through a 150 μm mesh sieve. Approximately two grams of powder was then uniaxially die pressed into 11.2 mm diameter pellets at a pressure of 16 MPa. After uniaxial pressing, the pellets were heated to 500 °C for 1 hour to remove water or other organic contaminants which might have been introduced during sieving or die pressing. Pellets were then isostatically pressed at 200 MPa.

The green density of the pellets was measured, after which they were then placed in a BN crucible, surrounded by a loose BN/AlN (50/50) bed. The pellets then were sintered under high purity N₂ (1 atm) in the previously mentioned graphite element resistance furnace at a temperature of 1850 °C for 100 minutes. After sintering, densities of sintered pellets were measured using Archimedes' principle according to ASTM standard C373-72. The pellets which had relatively high density, were sent to Virginia Polytechnic Institute and State University for thermal conductivity measurement.

4.7 ANALYSIS

Aluminum nitride powders were characterized by five different analytical methods: X-ray diffraction (XRD), particle size analysis (PSA), specific surface area measurement (SSA), scanning electron microscopy (SEM), and chemical analysis. The microstructure of sintered AlN pellets was examined by scanning electron microscopy and their thermal conductivities were measured.

4.7.1 X-ray Diffraction (XRD)

The nitrated powders were quantitatively phase analyzed using a Philips X-ray diffractometer (APD 1700). The powders were exposed to filtered CuK α radiation, at an accelerating voltage of 40 kV (\pm 0.1 %) and a beam current of 20 mA (\pm 0.1 %) with a scanning rate of 0.1 deg./sec. The intensity and 2θ data were acquired and stored using the Philips APD 1700 computer system. The raw data were corrected

for systematic error using AlN JCPDS-XRD pattern data as an internal reference standard. The intensity of the (100) hkl plane for AlN shown at 2θ of 33.2° and that of the (104) hkl plane for Al_2O_3 shown at 2θ of 35.2° were used. The details of the procedure used to quantify the XRD results are given in Appendix I.

4.7.2 Particle Size Analysis

The particle size and size distribution of the fully converted AlN powders were measured using the dynamic laser light scattering NICOMP 370, (Pacific Scientific Instrument Division). This instrument is capable of measuring particle diameters in the nanometre range. A small amount of AlN powder (< 0.5 g) was dispersed in ~ 15 mL distilled water and the soft agglomerated particles were broken down with an ultrasonic probe and dilute HCl added as a dispersant to adjust the liquid to $\text{pH} < 2$. The viscosity of the liquid was set to 0.933 cp (centipoise) for the instrument. About 20 ml of liquid was injected into the instrument. Light from a laser (5 mW HeNe) is focused into a glass tube or cuvet containing a dilute suspension of particles. Each of the particles illuminated by the incident laser beam scatters the incident light. The intensity of the light scattered by a single, isolated particle depends on its molecular weight, overall size and shape. By measuring the intensity of the scattered light, the mean spherical diameter of each particle can be calculated and displayed.

4.7.3 Specific Surface Area

Specific surface area of the powders was measured by the BET (Brunauer, Emmett and Teller) method²⁵ using a Quantachrome system (Quantasorb Sorption). The AlN powders (0.5 - 1 g of each) were loaded in pyrex glass sample holders (U shape tube), and then heated to 300 °C for 30 minutes to remove adsorbed water. After heating, N₂/He gas flows through the sample holder and then the powder is cooled down by liquid nitrogen. The volume of N₂ adsorbed is a function of the specific surface area of the powder. The process of adsorption and desorption are monitored by measuring the change in the thermal conductivity of the gas mixture.

4.7.4 Scanning Electron Microscopy

The morphology of AlN powders and the microstructure of sintered pellets were examined by scanning electron microscope (SEM) using JEOL T-300 and JEOL JSM 840A.

The powder samples were prepared by dispersing a small amount of AlN powder in ~15mL of acetone and the suspension ultrasonicated so as to break down the soft agglomerates. The dispersed powders were then placed on aluminum specimen mounts, dried and gold coated. The pellets of sintered AlN were sliced to ~3 mm thickness and mounted in bakelite. Mounted samples were ground and polished with diamond paste (1 μm particle size) and etched in 50 % HF solution for two minutes. Specimens were then gold coated. All microscopy specimens were sputter coated in a Hummer IV with an Au-Pd alloy for approximately 4 minutes.

4.7.5 Chemical Analysis

The oxygen and carbon contents in AlN powders were analyzed using the inert gas fusion method with a Strohlein Instrument CON-MAT 822 for oxygen analysis and a Leco Corporation Carbon Determinator (WR12) for carbon analysis. These tests were repeated at least four times for each sample.

Determination of some cation impurities was carried out by X-ray fluorescence using a Philips PW1400.

4.7.6 Thermal Conductivity Measurement

All thermal conductivity measurements of AlN specimens were carried out by Professor Hasselman at Virginia Polytechnic Institute using the laser-flash technique.

To prepare the samples for the thermal conductivity analysis, the AlN pellets were sliced to ~3 mm thickness and sputter coated with Au-Pd. This was done to prevent direct transmission of the laser beam through the specimen and to avoid detection of emitted radiation from the interior of the samples. In the laser flash technique, one side of the platelet-shaped specimen is subjected to a spatially uniform single pulse from a solid-state laser ($\lambda = 1.06 \mu\text{m}$). The transient temperature of the opposite face is monitored, usually by means of a remote optical sensor.²⁶ The thermal diffusivity is calculated using the thickness of the sample and the transient temperature. The thermal conductivity is then obtained from the thermal diffusivity using the specific heat capacity (C_p), $0.738 \text{ W}\cdot\text{sec./g}\cdot\text{K}$, which

was obtained from the technical bulletin of Keramont Corporation.

$$k = C_p \times \rho \times \delta \quad (4.1)$$

where k = thermal conductivity (W/m·K)

C_p = specific heat capacity (J/mol·K)

ρ = density of AlN pellet (kg/m³)

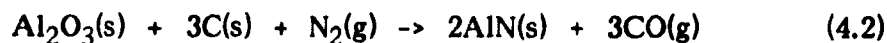
δ = thermal diffusivity (m/s)

4.8 THERMODYNAMIC MODELLING OF THE Al-N-O-C SYSTEM

4.8.1 Objectives of the Modelling

The objective of this modelling was to understand the thermodynamics of the reaction by which Al₂O₃, C, and N₂ react to produce AlN at high temperatures, using the Facility for the Analysis of Chemical Thermodynamics (F*A*C*T) system. The description of the F*A*C*T system and some of its programs can be found in Appendix II.

The overall reaction for the conversion of alumina to aluminum nitride is as follows:



The effect of excess C and N₂ on the product composition and changes to the predominance diagrams of Al-N-O-C system have been studied. It was suggested by Shanker et al.⁴ that the reaction may proceed via the two steps given in section 2.2.2 which involves the formation of the sub-oxide Al₂O₂ and CO₂. These reactions

were analyzed in the light of the assessed data existing on the F*A*C*T database.

4.8.2 Modelling Method

The thermochemical data of the reactants and products (shown in Appendix II) were assessed using the INSPECT program. Because the experimental reaction occurs using an excess of nitrogen (i.e. nitrogen gas flows during the reaction) the input into the EQUILB program was adjusted to account for this. All the possible products for the reaction of a given set of reactants at specified temperatures and pressures, along with various constraints at equilibrium were calculated by the EQUILB program. The gas solid reaction (2.4a) and the gas phase reaction (2.4b) were also scanned by the REACT program to find out which reaction was most likely to have occurred. It was assumed that the total pressure in the system was maintained at 1 atm.

The predominance diagrams were calculated by the PREDOM program using a constant nitrogen partial pressure (see below) but with varying CO and O₂ partial pressures. These partial pressures were based on the results of the above EQUILB study of carbothermal nitridation.

For this study, the reaction was simulated for 1 mole of Al₂O₃ (102 g) that reacts with 3 moles (stoichiometric ratio) or 6 moles (so as to simulate an excess of carbon) and 106.5 moles of nitrogen gas. Because, in most of experiments, 40 g of precursor material (Al₂O₃ : C > 1 : 6) was used, this material was a mixture of 23.44 g of Al₂O₃ (0.23 moles) and >8.27g of C (>0.69 moles). Nitrogen gas was

introduced into the furnace at a rate of 1.83 L/min. for 5 hours (total 549 liters of N₂ gas = 24.5 moles (S.T.P)). As stated above, this reaction was simulated for 1 mole of Al₂O₃, therefore, the amount of N₂ gas used as input into F*A*C*T was 106.5 moles (i.e. 24.5 moles N₂ / 0.23 moles Al₂O₃). Of this gas, only 1 mole of nitrogen was consumed during the reaction, therefore the remaining nitrogen gas was 105.5 moles (106.5 moles - 1 mole) and the amount of CO gas produced was 3 moles. Based on the above calculation, the partial pressures of nitrogen and CO in the product gases can be calculated as follows:

$$P(N_2) = 105.5 / (105.5 + 3) = 0.972 \text{ atm}$$

$$P(CO) = 3 / (105.5 + 3) = 0.0276 \text{ atm}$$

This result agrees with the partial pressures which are shown in Table 5.1 (in section 5.3) calculated using the EQUILB program. This was the gas composition used for the predominance diagram calculations.

CHAPTER 5: RESULTS AND DISCUSSION

5.1 EFFECT OF Al_2O_3 : C RATIOS ON CONVERSION

As stated earlier (Eq. 2.5) the stoichiometric ratio of Al_2O_3 : C is 1 : 3. To obtain full conversion of Al_2O_3 to AlN, excess carbon is usually required. The amount depends upon the reaction conditions, carbon source and mixing conditions, and will be described in this section.

A study to determine the minimum amount of excess carbon required for full conversion was carried out using a fine particle size ($0.025 \mu\text{m}$) boehmite ($\text{AlO}\cdot\text{OH}$, Bacosol 3C) and a coarser particle sized ($0.4 \mu\text{m}$) superground calcined Al_2O_3 (Alcoa, A16SG). Both cane sugar and carbon black were used as carbon sources. Figure 5.1 shows the effect of the Al_2O_3 : C molar ratio on conversion of Al_2O_3 to AlN for each combination of raw materials. The method used to calculate the ratio of Al_2O_3 : C for carbon from cane sugar is explained in Appendix III.

When cane sugar was used as a carbon source, full conversion of both α - Al_2O_3 (A16SG) and boehmite (Bacosol 3C) to AlN occurred with a Al_2O_3 : C of 1 : 3.2 which is close to the stoichiometric ratio of 1 : 3 as shown in Figure 5.1. However, when carbon black was used, the full conversion of both A16SG and Bacosol 3C to AlN was achieved only with an excess carbon black (Al_2O_3 : C > 1 : 4).

The reason for this difference in the degree of conversion is related to the intimacy of mixing. Cane sugar dissolves in water and coats all the available free surface of α - Al_2O_3 /boehmite particles prior to its conversion to carbon during

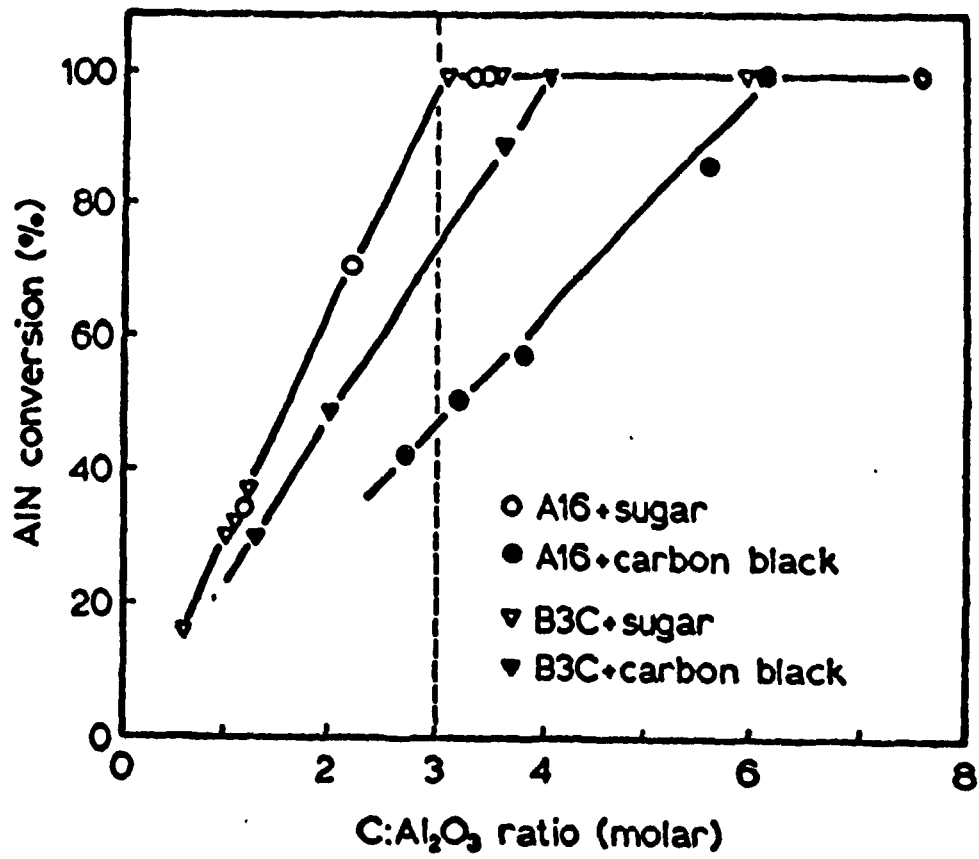


Figure 5.1: AIN conversion vs. Al₂O₃ : C ratio at 1600 °C for 5 hours.

pyrolysis. Therefore, every free surface of α - Al_2O_3 /boehmite can be coated by the carbon from cane sugar, so that full conversion to AlN could be achieved with a close-to-stoichiometric ratio of Al_2O_3 : C. The high degree of intimate mixing is also supported by the extent of conversion for sub-stoichiometric ratios (Figure 5.1). The amount of AlN formed is very close to theoretical when cane sugar was used as the carbon source.

Due to the lack of good mixing between the α - Al_2O_3 /boehmite and the carbon black, higher amounts of carbon were required to achieve full conversion to AlN. The solid-solid reaction (Eq.2.3), which is believed to be the main reaction in this carbothermal reduction, requires good physical contact between the Al_2O_3 and the C sources. Increasing the amount of carbon compensates for poorer mixing. The mechanism of the solid-solid reaction will be discussed in section 5.6.

Figure 5.1 also shows that the conversion rates of Bacosol 3C and A16SG were different when carbon black was used: full conversion to AlN from Bacosol 3C was achieved with a Al_2O_3 : C ratio of $\sim 1 : 4$ and full conversion from A16SG was achieved with $\sim 1 : 6$. This difference in the conversion rate could be caused by several factors: 1) reactivity difference between α - Al_2O_3 and boehmite, 2) particle size effect on the conversion rate, and 3) differences in mixing conditions in relation to the carbon source. It is known that the reactivity of boehmite is higher than α - Al_2O_3 .¹⁵ Also the particle size of Bacosol 3C (0.025 μm) is smaller than A16SG (0.4 μm). Thus when carbon black was used, because of poorer contact condition between the carbon black and α - Al_2O_3 /boehmite particles, the reaction rate could have been

more dependent on the reactivity and the particle sizes of Al_2O_3 source. Therefore, Bacosol 3C required less excess carbon than A16SG to achieve full conversion to AlN. However, as seen in Figure 5.1, there is no difference in the conversion rate between Bacosol 3C and A16SG when cane sugar was used. It is believed that the superior mixing of the carbon from cane sugar and $\alpha\text{-Al}_2\text{O}_3$ /boehmite overcomes the differences in the reactivity and particle size of different type of Al_2O_3 source.

The use of cane sugar as a carbon source leads to full conversion to AlN for both $\alpha\text{-Al}_2\text{O}_3$ and boehmite with a close-to-stoichiometric ratio of $\text{Al}_2\text{O}_3 : \text{C}$ due to the superior mixing conditions. Accordingly, cane sugar was used in all following experiments.

5.2 EFFECT OF REACTION TEMPERATURE ON CONVERSION

A series of experiments to optimize the reaction temperature was carried out using boehmite (Bacosol 3C) and $\alpha\text{-Al}_2\text{O}_3$ (A16SG), with cane sugar as the carbon source. The ratio of $\text{Al}_2\text{O}_3 : \text{C}$ was held constant at 1 : 3.5, i.e. the carbon having slightly in excess to ensure conversion. All raw materials were ball milled for 18 hours, carburized, and then nitrided for 5 hours at varying reaction temperatures.

As seen in Figure 5.2, the extent of normalized conversion rate (wt. fraction / precursor mass x reaction time) of both $\alpha\text{-Al}_2\text{O}_3$ and boehmite increased with reaction temperature with full conversion to AlN being obtained at $\geq 1600^\circ\text{C}$. Figure 5.2 also shows that the degree of reaction was higher for $\alpha\text{-Al}_2\text{O}_3$ than for boehmite and as the reaction temperature increased the difference in the degree of reaction

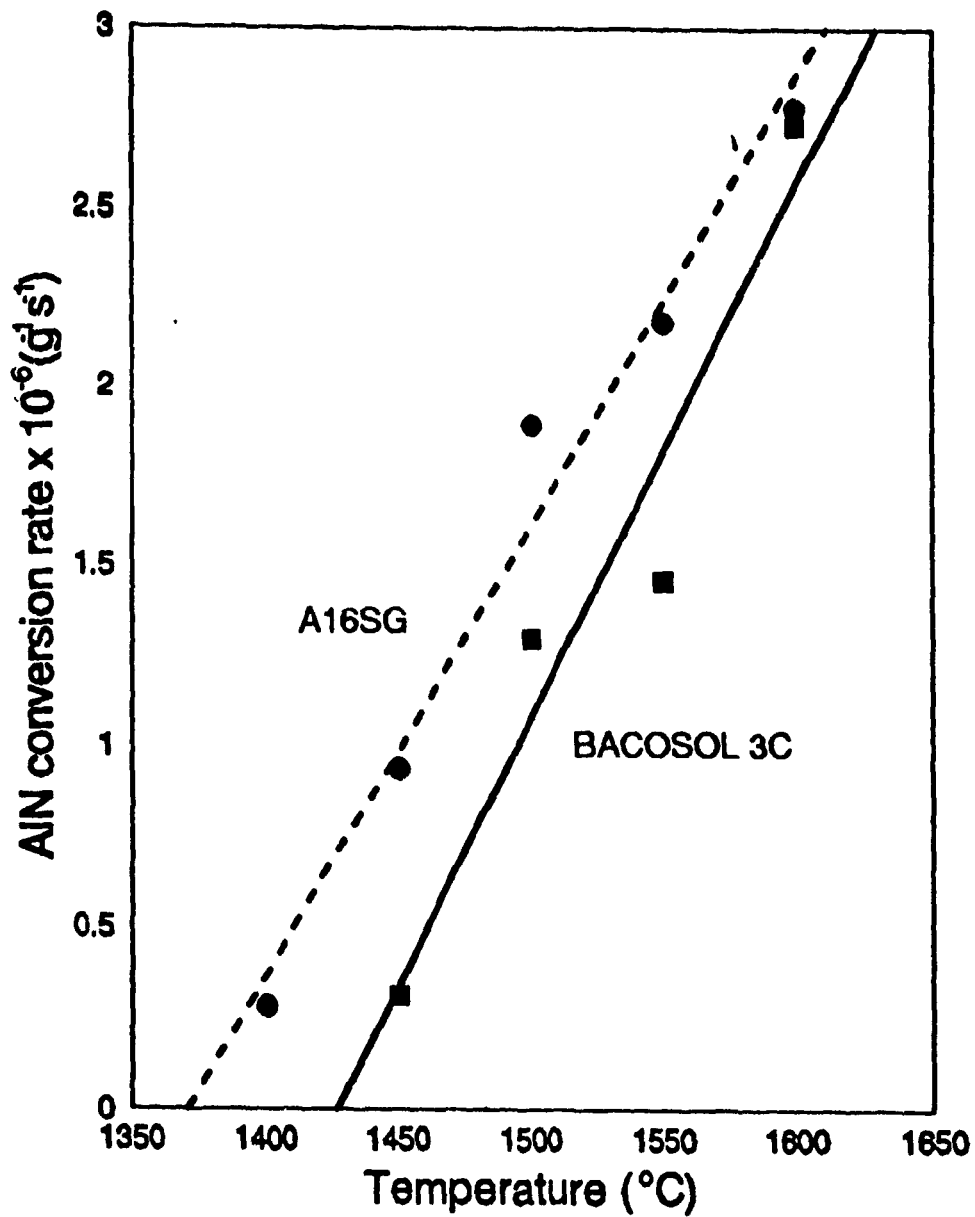


Figure 5.2: AIN conversion rate vs. reaction temperature (reaction time of 5 hours) using Bacosol 3C and A16SG and cane sugar as a carbon source. ($\text{Al}_2\text{O}_3 : \text{C} = 1 : 3.5$)

decreased. It is believed that the degree of reaction is affected by the combined effects of reaction temperature, time, carbon source, morphology and reactivity of the Al_2O_3 source which relate to the particle/agglomerate size of the Al_2O_3 precursor. In this section of experiments, all reaction conditions were the same, except for the Al_2O_3 . The reactivity of Bacosol 3C is expected to be higher than that of A16SG¹⁵. Moreover, the particle size of Bacosol 3C (0.025 μm) is smaller than that of A16SG (0.4 μm). However, the result of NICOMP particle size analysis (section 5.5) indicates that Bacosol 3C contains ~80 volume % of ~0.6 μm sized agglomerated particles even after 18 hours of post-reaction ball milling. These larger agglomerated particles would decrease the conversion rate of Bacosol 3C to less than that of A16SG α - Al_2O_3 in spite of Bacosol 3C having a higher reactivity and smaller particle size. This is supported by the activation energy values calculated from the experimental data for Bacosol 3C and A16SG (Figure 5.3). Figure 5.3 shows the slopes of \ln conversion rate vs. $1/T$ for both Bacosol 3C and A16SG which gives the activation energy for the conversion to AlN. The activation energy calculated for Bacosol 3C and A16SG are 365.6 kJ/mole and 257.4 kJ/mole, respectively. According to the plotted lines in Figure 5.3, the reaction constant for Bacosol 3C and A16SG ($K_{\text{O}B3C}$, $K_{\text{O}A16}$) can be determined to be 4.1×10^{-7} and 1.4×10^{-6} , respectively, and the following expressions can be derived:

$$K_{B3C} = 4.1 \times 10^{-7} \exp(-365.6 \text{ kJ/RT})$$

and

$$K_{A16SG} = 1.4 \times 10^{-6} \exp(-257.6 \text{ kJ/RT}).$$

These activation energy values for Bacosol 3C and A16SG are comparable to those

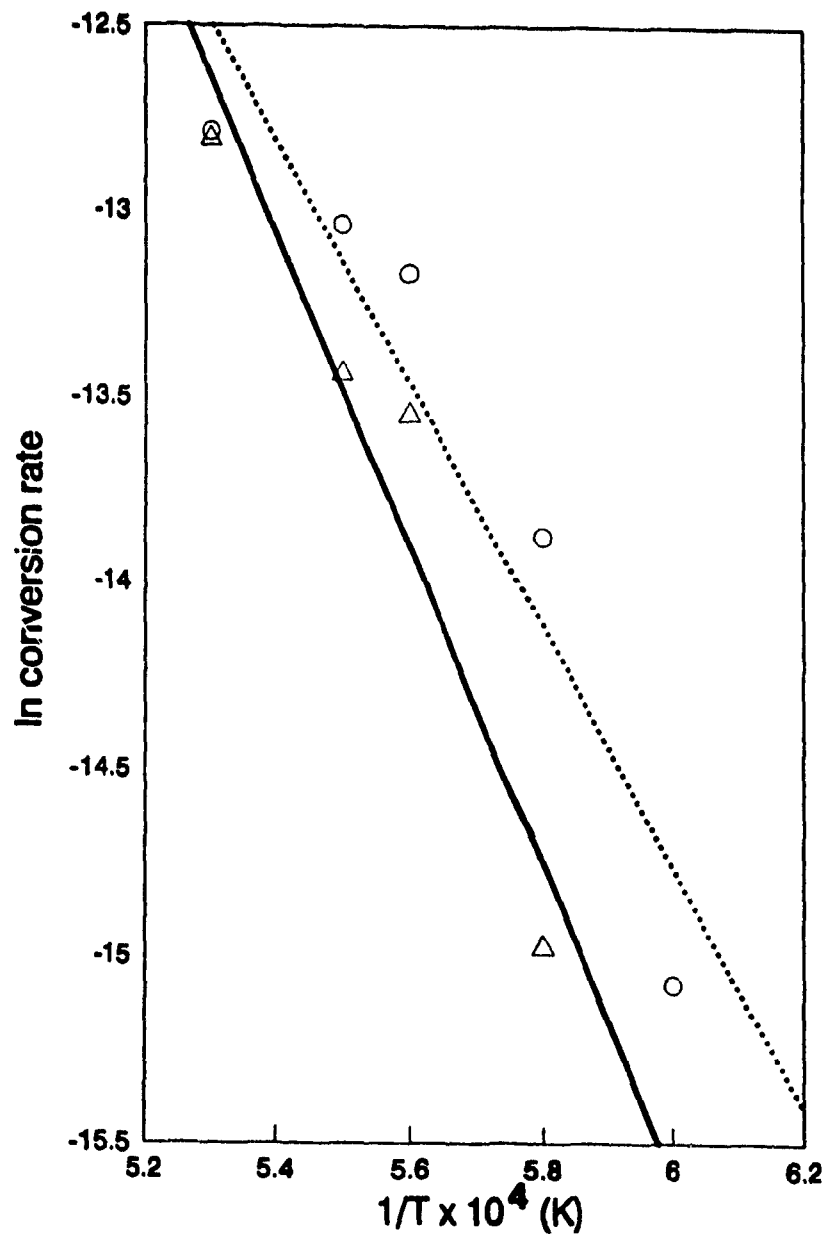


Figure 5.3: The Arrhenius plot of \ln (wt. fraction / (precursor material wt. \times reaction time)) vs. $1/T$ for Bacosol 3C and A16SG

determined for the O_2 lattice diffusion in Al_2O_3 (238 - 636 kJ/mole).²⁶ Thus, the experimental values are not inconsistent with solid state diffusion of these species occurring as the rate determining step during the carbothermal reduction of Al_2O_3 to AlN.

Figures 5.4 (a), (b), (d) and (e) show the morphology of AlN powder produced using Bacosol 3C after carbothermal reduction at 1550 °C, 1600 °C and 1650 °C. These powders were decarburized at 720 °C for 5 hours to remove the excess carbon.

Figure 5.4 (a) shows the mixture of AlN and unreacted Al_2O_3 and Figure 5.4 (b) shows particles of unreacted Al_2O_3 which were present in the final powder after reaction at 1550 °C, also confirmed by EDS analysis (Figure 5.4(c)). The products after the reaction at 1600 °C and 1650 °C contained only AlN according to X-ray analysis. There is, however, a difference in the degree of agglomeration. AlN powder produced at 1600 °C (Figure 5.4 (d)) has smaller agglomerate sizes (0.2 μm) than those produced at 1650 °C. This is due to sintering of Al_2O_3 prior to nitridation and/or sintering of fine AlN crystallites. Sintering of Al_2O_3 is done at temperatures of 1450 - 1650 °C and sintering of AlN is typically done at 1650 - 1850 °C^{3,5,24}. The extent of sintering of agglomerated Bacosol 3C would increase with increasing reaction temperature, with almost complete sintering of the agglomerated boehmite particles occurring at temperatures ≥ 1600 °C. Moreover, the reaction temperature of 1650 °C would have been enough to sinter fine AlN particles which were close to each other. Therefore, it is believed that most of the AlN agglomerates were caused

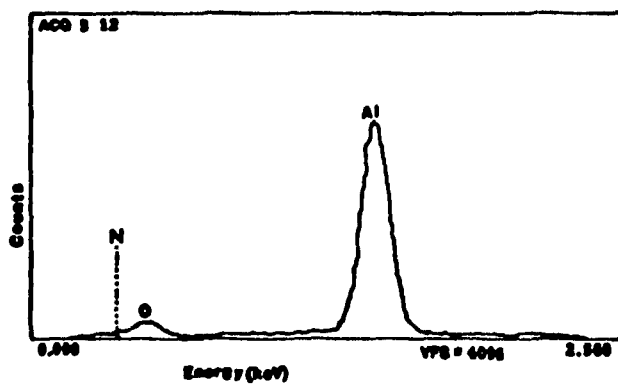
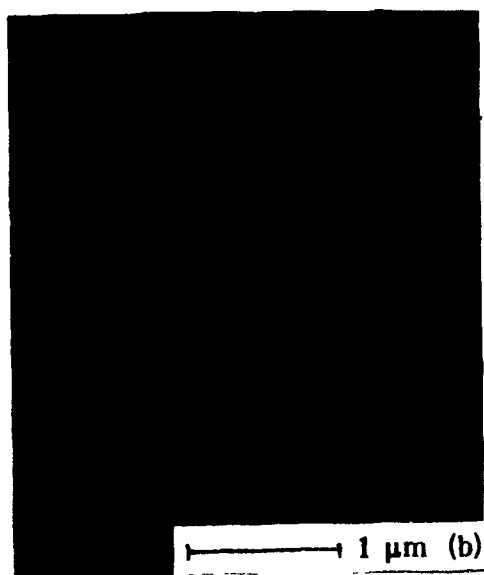
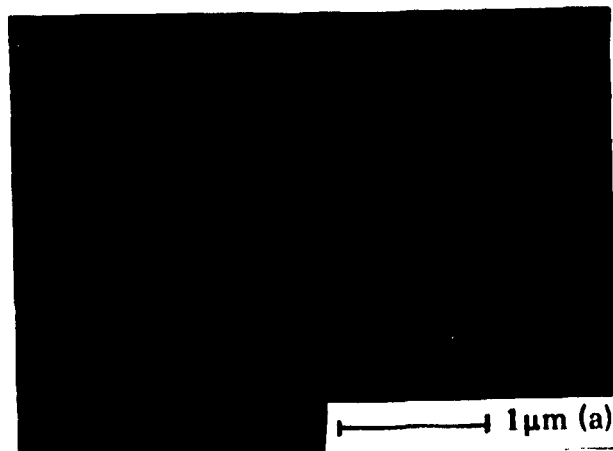


Figure 5.4: Micrograph of AlN powder nitrided from Bacosol 3C at 1550 °C, (a) mixture of AlN and Al₂O₃, (b) unreacted Al₂O₃ and (c) EDS analysis of (b) showing O₂ peak

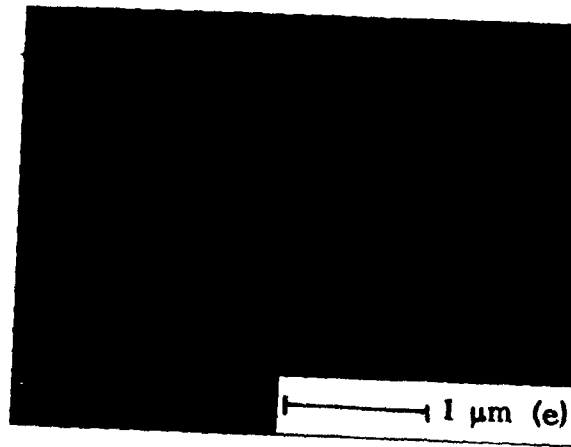
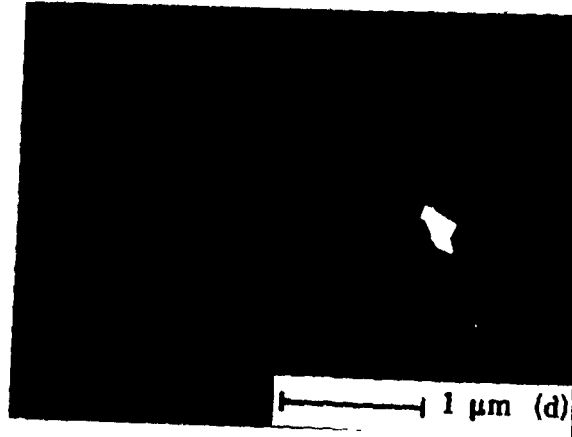


Figure 5.4: Micrograph of fully converted AlN powder nitrided from Bacosol 3C at (d) 1600 °C, and (e) 1650 °C.

by sintering of Al_2O_3 prior to nitridation at reaction temperatures of 1600 °C and 1650 °C. Also, more extensive AlN agglomeration was found after nitridation at 1650 °C as a result of sintering. Hence, to minimize sintering while achieving full conversion, it is necessary to maintain the reaction temperature at 1600 °C, particularly for fine starting materials.

5.3 THERMODYNAMIC MODELLING OF Al-O-N-C SYSTEM

The overall reaction of carbothermal reduction is as follows:



It has been suggested by Shanker et al.¹⁴ that this reaction may proceed via several possible gas phase reactions:



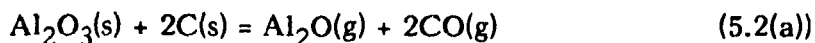
and



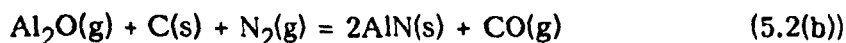
Another possible reaction to form AlN from Al_2O_2 may be



It can also be thought that the gas phase reaction may occur in the presence of Al_2O gas:



and



Similarly, another possible reaction to form AlN from Al_2O may be:

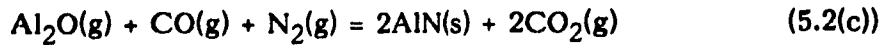


Table 5.1 shows the change of Gibbs energy (ΔG) obtained from the REACT program for the reactions written above for the temperature range of 1500 - 1700 °C. The change of Gibbs energy for the reactions (5.1(a) and 5.2(a)) forming suboxide gases (Al_2O_2 and Al_2O) are positive, 426 - 480 kJ and 232 - 313 kJ respectively in the range of reaction temperatures studied (1500 - 1650 °C). Thus, it is very unlikely

Table 5.1: The Gibbs energy change for the possible reactions of carbothermal reduction of Al_2O_3 to AlN

T(°C)	$\Delta G(\text{kJ})$						
	5.1	5.1(a)	5.1(b)	5.2(a)	5.2(b)	5.1(c)	5.2(c)
1500	64	480	-415	313	-249	-140	-111
1550	47	461	-415	286	-239	-122	-93
1600	30	444	-414	259	-229	-105	-75
1650	13	426	-414	232	-220	-87	-57
1700	-4	408	-413	206	-210	-70	-39

that Al_2O_2 or Al_2O gas will form and react with C(s) or CO(g) even though the reactions, which form AlN from these sub-oxide gases, have negative ΔG values. The ΔG for the overall reaction (5.1), which is the solid state reaction, is also positive, 13 - 64 kJ in the range of reaction temperatures (1500 - 1650 °C). However, as temperature increases ΔG decreases and when the temperature exceeds 1700 °C it becomes slightly negative. The reason that AlN can be formed at all at the reaction temperature used in this study is believed to be due to the use of excess N_2 gas.

This excess gas dilutes the product gases and force the solid state reaction (5.1) to proceed forward.

Table 5.2 shows the partial pressures of N_2 , CO, CO_2 , Al_2O_2 and O_2 calculated by the EQUILIB program for the reaction of the stoichiometric ratio of $Al_2O_3 : C$ and one at the experimental non-stoichiometric ratio of $Al_2O_3 : C$ (1 : 6) at 1600 °C. The amount of N_2 (106.5 moles) as input into the EQUILIB program was calculated based on the total amount of N_2 introduced over a reaction time of five hours (see section 4.8.2). Table 5.2 also shows that Al_2O_2 , O_2 and CO_2 gas are present under all reaction conditions, however, the concentrations of these gases are negligible relative to those of N_2 and CO.

Table 5.2. Partial pressures of N_2 , CO, CO_2 , Al_2O_2 and O_2 for the equations of $Al_2O_3 + 3C + 106.5N_2$ and $Al_2O_3 + 6C + 106.5N_2$ at 1600 °C

C (mole)	P(N_2) (atm)	P(CO) (atm)	P(CO_2) (atm)	P(Al_2O_2) (atm)	P(O_2) (atm)
3	0.972	0.276E-1	0.968E-7	0.153E-13	0.228E-17
6	0.972	0.277E-1	0.370E-7	0.223E-14	0.334E-18

Figures 5.5 (a) and (b) show the changes of partial pressures of N_2 , CO and O_2 as the N_2 gas input increases. Similar graphs for $P(Al_2O_2)$ and $P(CO)$ can be found in Appendix II. From Figure 5.5, it can be seen that as the N_2 gas increases, $P(CO)$ and $P(O_2)$ decrease due to dilution. It is also found that as the temperature increases, $P(N_2)$ and $P(CO)$ do not change significantly, but $P(O_2)$ increases slightly, as shown in Figure 5.6, although the absolute increases are small and the EQUILIB

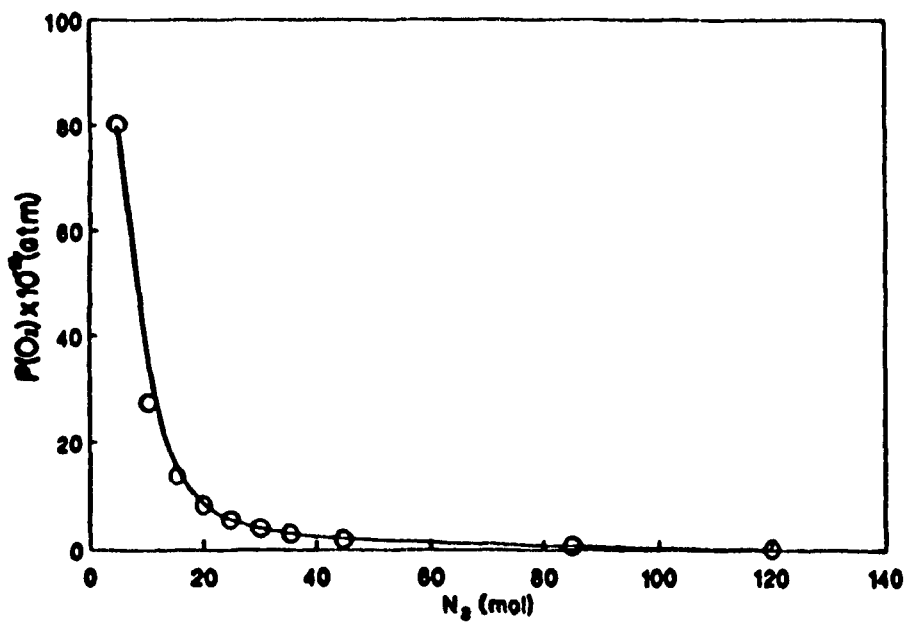
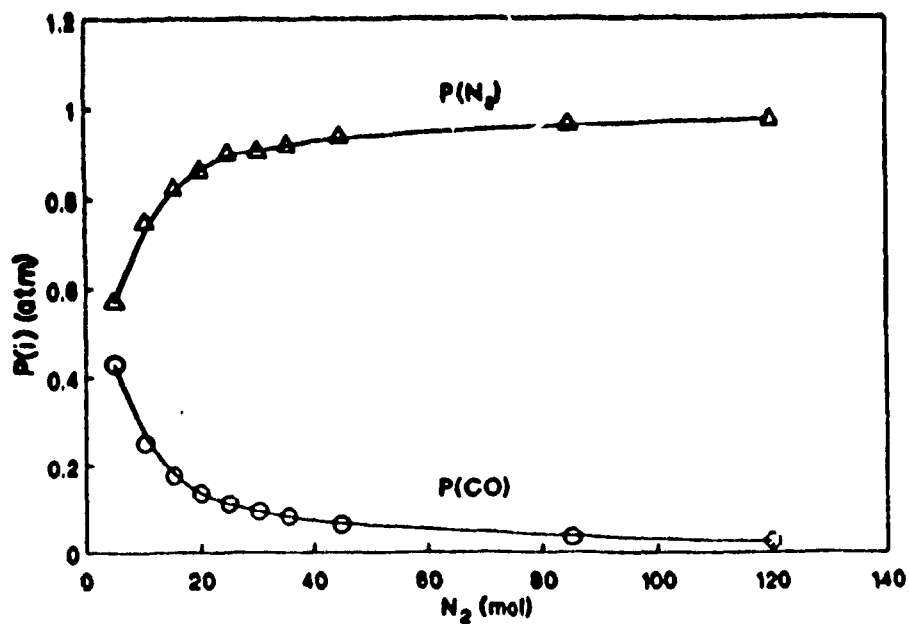


Figure 5.5: (a) Partial pressure of N_2 and CO vs. amounts of N_2 gas introduced and (b) Partial pressure of O_2 vs. amounts of N_2 gas introduced, at $1600^\circ C$ ($Al_2O_3 : C = 1 : 6$)

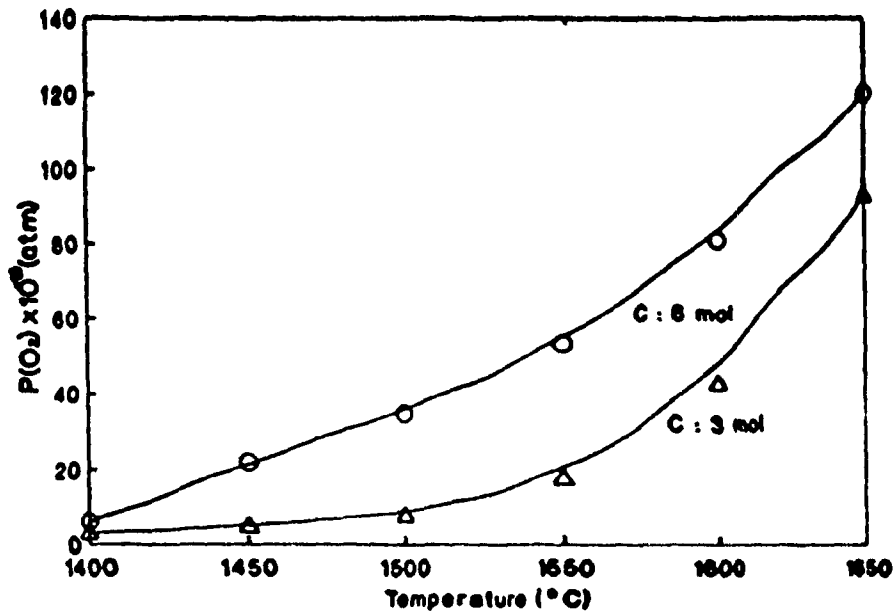


Figure 5.6: Partial pressure of O₂ as a function of reaction temperature and Al₂O₃ : C ratio

calculations indicate that this would not interfere with the conversion to AlN.

For the stoichiometric Al₂O₃ : C ratio of 1 : 3 at 1600 °C, the EQUILIB calculations also indicates full conversion of Al₂O₃ to AlN. However, it is well established that this is not the case during carbothermic synthesis. The reasons for this discrepancy are kinetic considerations which are not possible to model using the F*A*C*T system since the EQUILIB program calculations assume perfect mixing of the reactants and is time independent.

The effect of N₂ is to dilute the concentration of CO and O₂ to low levels

thus allowing the full conversion to AlN. This situation can be represented by a predominance diagram. Figure 5.7 (a) and (b) are composite Al-N-O-C system predominance diagrams indicating the major phases present as a function of $P(O_2)$ and $P(CO)$ for the temperature range of 1400 - 1700 °C. In all cases, the $P(N_2)$ is maintained constant at 0.972 atm (see Table 5.2). When the partial pressure of CO is higher than 10^3 atm, $Al_4C_3(s)$ is present below 1550 °C and when the partial pressure of CO is higher than $10^{13.5}$ atm AlC(g) forms above 1600 °C. Also when the partial pressure of O_2 is very high ($> 10^{15}$ atm), $Al_2O_3(s)$ is present for the whole range of temperatures. In the low temperature range (1450 -1550 °C), as temperature increases, the boundary between AlN and Al_4C_3 shifts to lower partial pressure of CO gas range, as shown Figure 5.7 (a). In high temperature range, $Al_4C_3(s)$ disappears and AlC(g) appears, and as the temperature increases the boundary of AlN and AlC shifts to lower partial pressures of CO gas, as shown in Figure 5.6 (b).

In Figure 5.7 (a) and (b), the partial pressures of CO and O_2 calculated by the EQUILIB program are plotted for both the stoichiometric $Al_2O_3 : C$ ratio of 1 : 3 and the higher $Al_2O_3 : C$ ratio of 1 : 6 at 1500 °C and 1600 °C. These points are in the region of AlN indicating that only AlN would occur under these conditions. Furthermore, during the actual synthesis experiments, carried out under conditions of flowing nitrogen, all the product gases would be purged from the system. Therefore, the actual partial pressures of CO and O_2 in an open system must be even lower than the values calculated by the EQUILIB program for a closed system

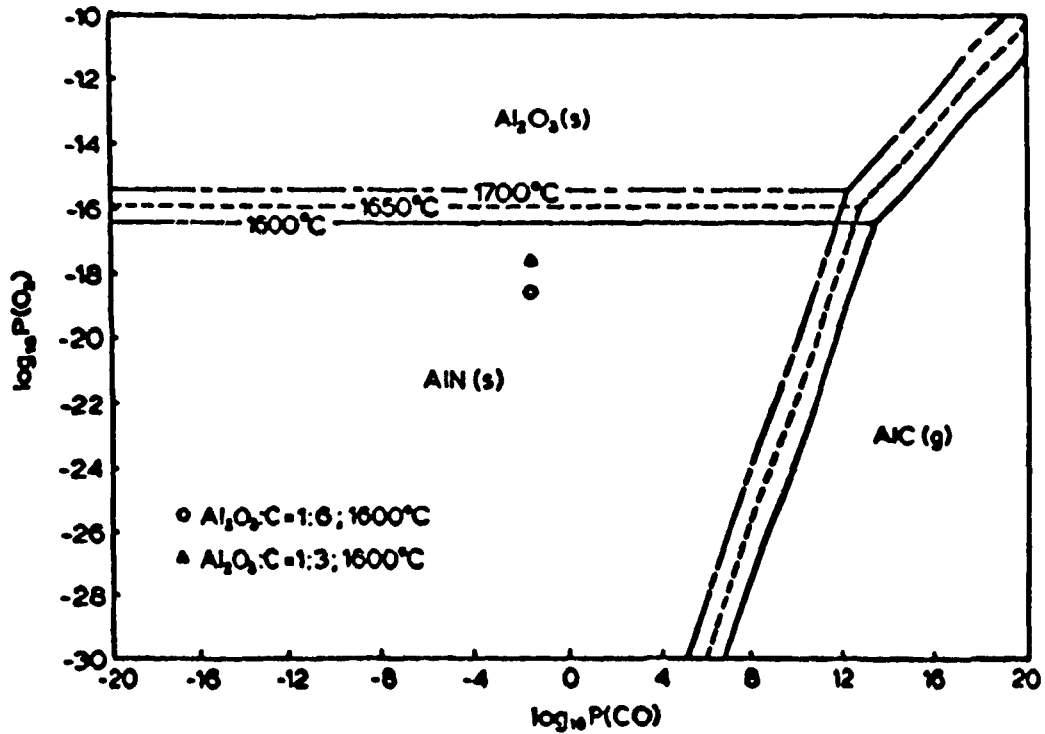
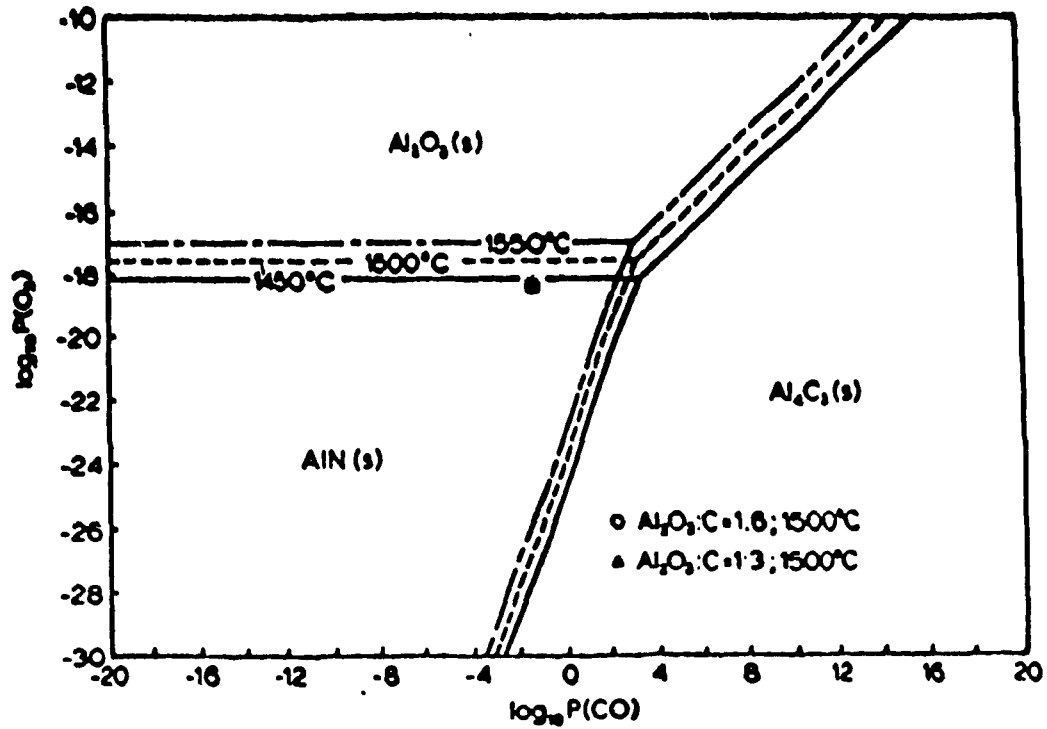


Figure 5.7: Combined predominance diagrams of the Al-N-O-C system (a) at 1450 °C, 1500 °C and 1550 °C and (b) at 1600 °C, 1650 °C and 1700 °C. $P(O_2)$ vs. $P(CO)$, $P(N_2)$ is constant at 0.972 atm

and the possibility of forming AlC or Al₄C₃ would be extremely low. It is shown that the equilibrium partial pressures of CO and O₂ in Figure 5.7 (a) is closer to the boundary of Al₂O₃ and AlN at 1550 °C than at 1600 °C in Figure 5.7 (b). This indicates that there is a greater possibility for unreacted Al₂O₃ to remain in the powder nitrided at 1550 °C than 1600 °C, which supports the results of the reaction temperature study discussed in section 5.2.

Based on the thermodynamic study, the following conclusions can be drawn:

- (1) positive ΔG values for suboxide formation (Al₂O₂, Al₂O) and low partial pressure of these species precludes their participation in the carbothermal nitridation process and it is extremely unlikely that they partake in any intermediate step in the reaction process,
- (2) there is no possibility of aluminum carbide formation (Al₄C₃, AlC) under the experimental conditions described in this thesis,
- (3) the ability to form AlN from Al₂O₃ is driven by the presence of N₂ gas which, under experimental conditions, flushes out the product gas (CO) and thus forces the equilibrium in favour of AlN formation, assuming the P(O₂) is maintained at a low level.

5.4 EFFECT OF REACTION TIME ON CONVERSION

To study the effect of reaction time, two types of Al₂O₃ and one boehmite were used: θ -Al₂O₃ (0.07 μm , T40X), α -Al₂O₃ (0.3 μm , HPA-0.5) and boehmite (0.025 μm , Bacosol 3C). The ratio of Al₂O₃ : C and reaction temperature for this

series of experiments were 1 : ~3.5 and 1600 °C. In addition, another series of experiments was performed with T40X at 1500 °C with the same ratio of Al₂O₃ : C, for comparison with the results at higher temperature.

Figure 5.8 shows the conversion rates for each starting material as a function of reaction time. A time of zero hours is defined as the time at which the furnace reached 1600 °C. Heating and cooling rates were similar and the furnace took about 7.5 minutes to go from 1450 °C to 1600 °C. The amount of converted AlN with a reaction time of zero hours was 81 % AlN for T40X, 44 % for Bacosol 3C and 4 % for HPA-0.5 (Figure 5.8). The minimum reaction time for achieving full conversion to AlN was 0.33 hours for T40X, 1.5 hours for HPA-0.5 and two hours for Bacosol 3C.

The rapid conversion of T40X (θ -Al₂O₃) is believed to be due to its fine particle size (0.07 μ m) and good dispersion characteristics (section 5.5). On the other hand, because the agglomerates of Bacosol 3C were hard to break down, the degree of conversion was lower than that of T40X, even though the reactivity of boehmite (Bacosol 3C) is recognized to be higher than that of θ -Al₂O₃ (T40X).¹⁵ Furthermore, the large agglomerated particles of Bacosol 3C (~0.6 μ m) resulted in a slower rate of conversion to AlN than HPA-0.5, which has a narrow particle size distribution (d = ~0.3 μ m). Consequently HPA-0.5 converts more uniformly and reaches full conversion in less time than Bacosol 3C. Particle size distributions are discussed in more detail in the next section.

The results presented here show that the conversion rate for each Al₂O₃

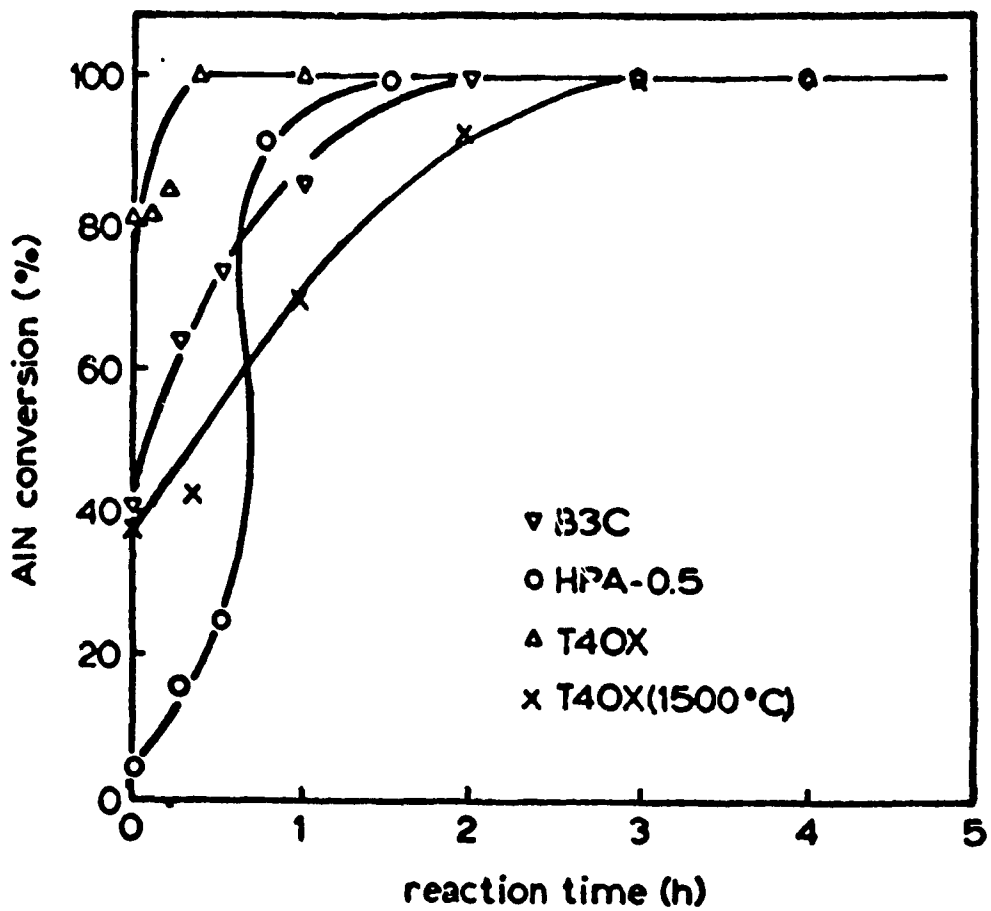


Figure 5.8: Percent AIN conversion for Bacosol 3C, T40X, and HPA-0.5 as a function of reaction time at 1600 °C (at 1500 °C for T40X) and Al₂O₃ : C = 1 : 3.5 with cane sugar as a carbon source

source can be affected by the particle/agglomerate size effect and the variable reactivity of the different types of Al_2O_3 , i.e. whether it is a hydrated or not. Furthermore, the degree of agglomeration of particles can also affect the conversion rate, i.e. even if the Al_2O_3 source has a fine ultimate particle size, if its degree of agglomeration prior to reaction is high, the conversion rate is lower. It is believed that these factors combine synergistically and affect the conversion rates of each raw material; i.e. the conversion rates for each Al_2O_3 source do not simply reflect either its particle size or reactivity but apparently these work in combination.

Figure 5.8 also shows the amount of converted AlN with a lower temperature (1500 °C) for T40X: 40 % and 50 % for a reaction time zero hours and 0.33 hours respectively, which are approximately half the conversion observed at 1600 °C. Furthermore, full conversion to AlN was realized for a longer reaction time of three hours (versus 20 minutes at 1600 °C). The lower reaction temperature clearly causes slower reaction kinetics, hence, the conversion rate was lower and the minimum reaction time for full conversion to AlN was longer than that carried out at 1600 °C.

5.5 RELATIONSHIP BETWEEN THE PARTICLE/AGGLOMERATE SIZES OF THE PRECURSOR Al_2O_3 AND AlN PRODUCT WITH REACTION TIME

Figure 5.9 (a) - (c) shows the particle and agglomerates sizes of the AlN powders produced using Bacosol 3C, T40X, and HPA-0.5 as a function of reaction

time. These data were obtained on the NICOMP particle size analyzer. Each data point represents the average particle size from 5 - 8 of separate analyses for each powder. The smallest particle size groups in Figure 5.9 for each AlN powder represents the average particle sizes for the individual AlN powder grains and the larger size fraction groups represents the average hard agglomerate size. Each bar in Figure 5.9 represents the distribution range of average particle/agglomerate size for the analysis. From Figure 5.9, it can be seen that no significant change in particle or agglomerate size is observed as a function of reaction time for all of the AlN powders.

Figure 5.10 (a) - (c) shows typical examples of particle size distribution graphs for AlN powders produced using Bacosol 3C, T40X, and HPA-0.5 provided by the NICOMP particle size analyzer. An examination of Figures 5.10 will show that the AlN powders produced using Bacosol 3C and T40X show trimodal particle size distributions: $\sim 0.05 \mu\text{m}$ sized particles, particles between $0.1 \mu\text{m}$ and $0.7 \mu\text{m}$, and particles $> 1 \mu\text{m}$. The largest group of particle sizes of these two AlN powders are not shown in Figure 5.9 because it is believed that this size fraction represents soft agglomerates, which can be broken down easily by milling. This was supported by the large shift in the mean size of this particle size grouping from analysis to analysis on the same powder. The AlN powder produced using HPA-0.5 shows only a bimodal particle size distribution: sub-micron sized particles between $0.3 \mu\text{m}$ and $0.9 \mu\text{m}$ and $> 1 \mu\text{m}$ sized hard agglomerated particles (see Figure 5.10 (c)).

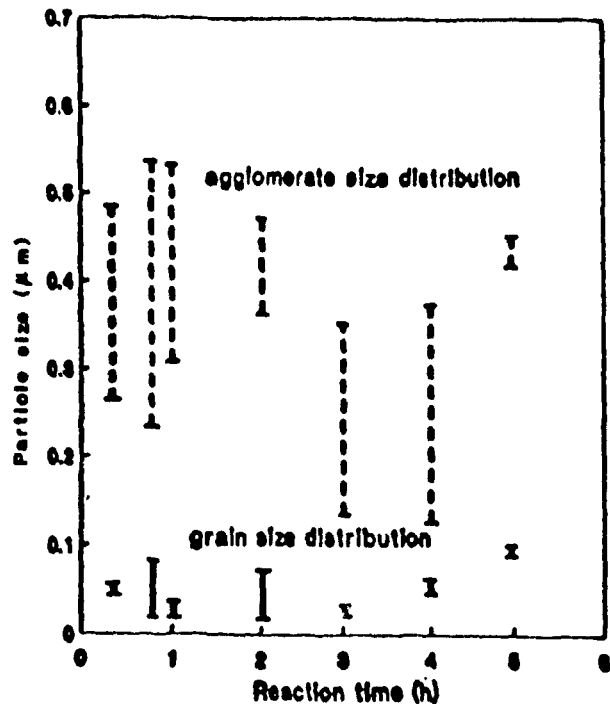
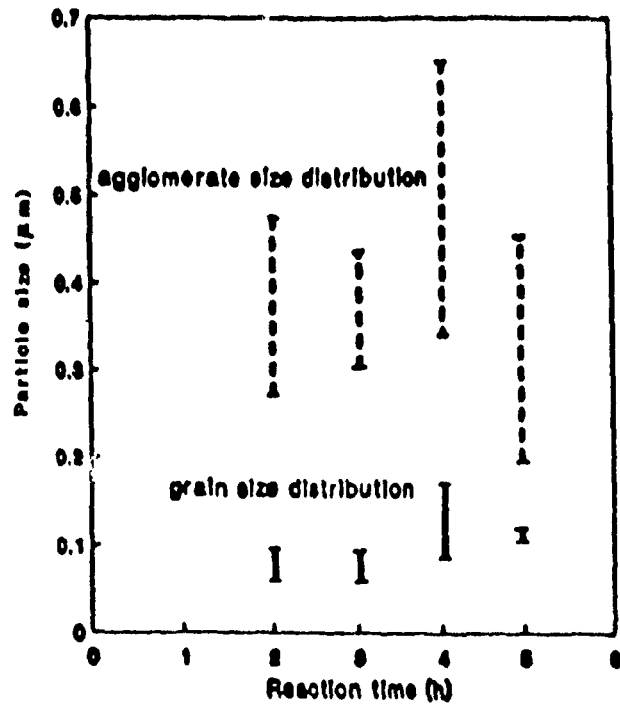


Figure 5.9: Variation in particle sizes of the AlN powders produced using (a) Bacosol 3C and (b) T40X as a function of reaction time at 1600 °C.

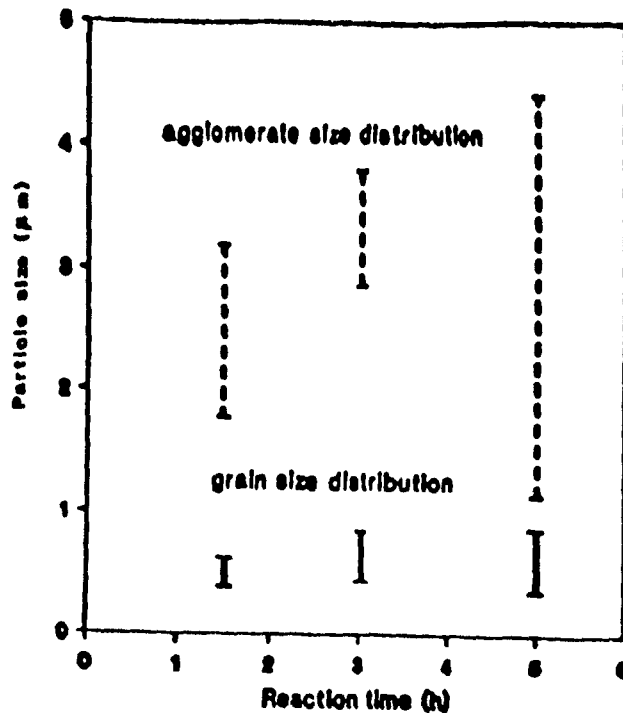


Figure 5.9: (c) Variation in particle sizes of the AlN powders produced using HPA-0.5 as a function of reaction time at 1600 °C.

It is believed that the hard agglomerates observed in the AlN powders are the result of: (1) sintering of Al_2O_3 agglomerates during nitridation, but prior to conversion to AlN and (2) partial sintering of AlN powders after complete nitridation. Since the reaction temperature was high relative to the sintering temperature of Al_2O_3 (1400 -1650 °C), Al_2O_3 agglomerates in the precursor would have sintered. On the other hand, the sintering of converted fine AlN powders could also have caused the agglomeration. Troczynski et al.²³ have observed that fully

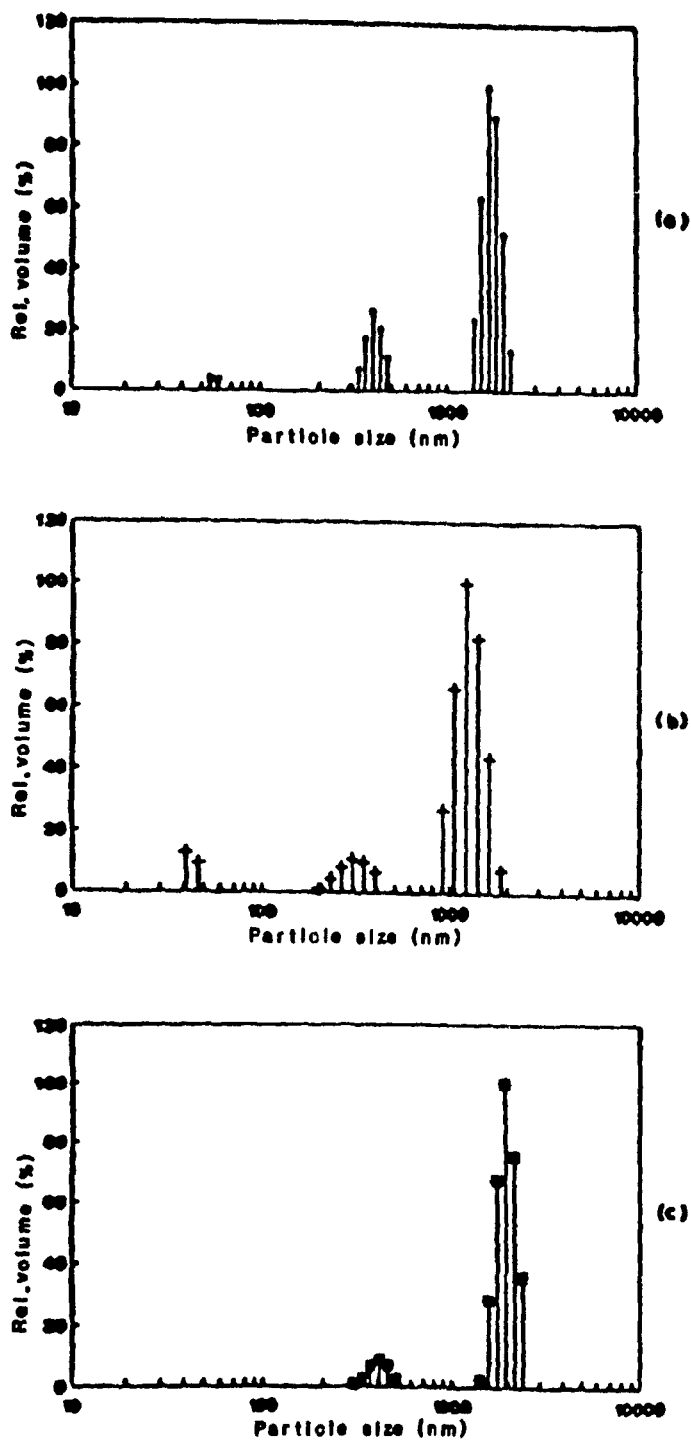


Figure 5.10: Typical example of particle size distribution graphs of AlN from (a) Bacosol 3C, (b) T40X and (c) HPA-0.5 provided by the NICOMP particle size analyzer.

dense sintered AlN, without sintering aid, was achieved at 1800 °C whereas sintering at 1600 °C resulted in only ~60 % of theoretical density being achieved. Since the reaction temperature was 1600 °C and the powders were not compacted, only fine, adjacent AlN particles could have sintered partially. In any case, weak agglomeration of this type could easily be broken down by milling after decarburization.

To compare the morphology of AlN powders produced under the same reaction conditions, different types of Al₂O₃ sources were reacted: α-Al₂O₃ (A16SG, HPA-0.5), γ-Al₂O₃ (Alumina Sol P-3), θ-Al₂O₃ (T40X) and boehmite (Bacosol 3C, Pural 200). Table 5.3 shows the particle sizes obtained from NICOMP analysis data of AlN powders produced using these different Al₂O₃ sources with cane sugar as the carbon source. Data for two commercial AlN powders are also included. The different morphologies of these AlN powders are shown in Figure 5.11. These micrographs show the different particle sizes of AlN particles as well as their particle size distributions. The different extent of agglomeration of the powders is also clearly indicated.

As shown in Figure 5.11, the AlN powder morphology of (a) HPA-0.5 and (b) A16SG is similar to that of (g) Tokuyama Soda which has narrow particle size distribution. The micrographs of two boehmite-derived powders ((c)Bacosol 3C and (d) Pural 200) show wide distribution of particle size, with a range from sub-micron to around one micron sized particles. This is, as discussed above, believed to be due to the agglomeration of the boehmite and sintering problems prior to conversion.

Table 5.3: AlN powder characteristics produced from different precursors
(1600 °C, 5 hours, Al₂O₃ : C = 1 : 6)

	TYPE OF Al ₂ O ₃ SOURCE	PRECURSOR PARTICLE SIZE (μm)	AlN PARTICLE SIZE (μm)
Alumina Sol P-3	γ-Al ₂ O ₃ [#]	0.02	0.3
Bacosol 3C	boehmite	0.025	0.085
Pural 200	boehmite	0.038	0.053
T40X	θ-Al ₂ O ₃ [#]	0.07	0.092
HPA-0.5	α-Al ₂ O ₃	0.3	0.36
A16SG	α-Al ₂ O ₃	0.4	0.54
COMMERCIAL AlN			
STARCK C [*]	N/A	N/A	0.2
TOKUYAMA SODA ⁺	N/A	N/A	0.3

[#]: supplier's data

^{*}: produced by direct nitridation

⁺: produced by carbothermal reduction

The micrograph of the AlN powder from (e) T40X θ-Al₂O₃ also shows a wide distribution of particles size. In the micrograph of (f) SOL-P3 γ-Al₂O₃, many of the 0.2 - 1 μm sized particles are seen despite the fact that this was the finest powder used in the study (< 0.02 μm). Again, the micrograph of this powder shows extensive agglomeration of fine particles due to sintering of Al₂O₃ particles prior to the reaction.

Table 5.3 shows that fine Al₂O₃ precursors (T40X, Bacosol 3C, Pural 200) produced fine AlN powders whereas coarse Al₂O₃ sources (A16SG, HPA-0.5) produced coarse AlN. For example, Pural 200 boehmite (0.038 μm) produced

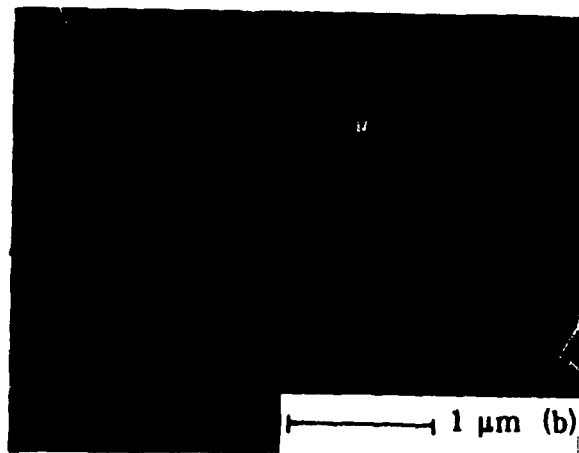
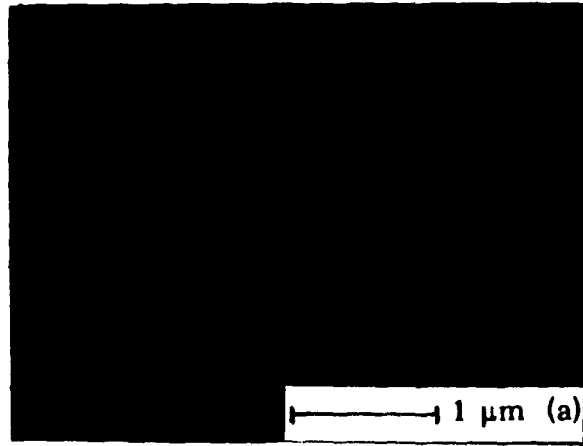


Figure 5.11: Micrographs of AlN powders produced using α -Al₂O₃ (a) HPA-0.5 and (b) A16SG with cane sugar as a carbon source at 1600 °C for five hours

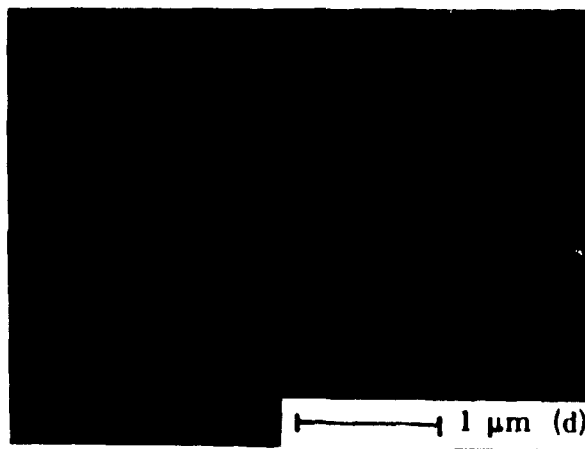
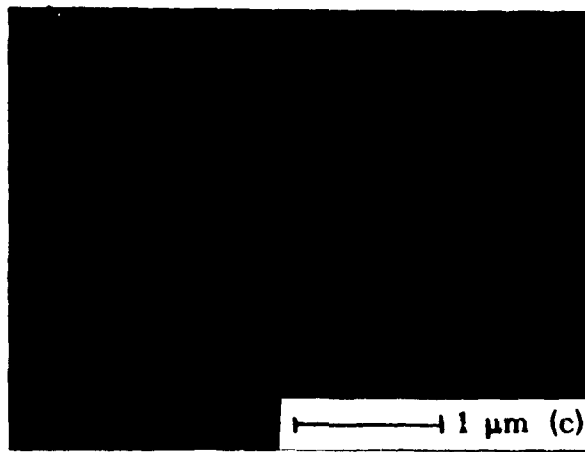


Figure 5.11: Micrographs of AlN powders produced using boehmite (c) Bacosol 3C and (d) Pural 200 with cane sugar as a carbon source at 1600 °C for five hours

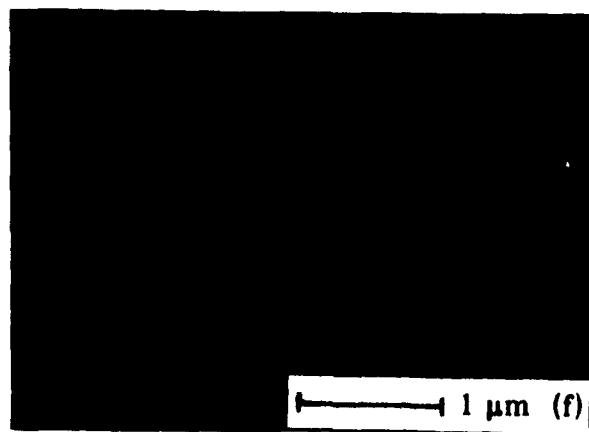
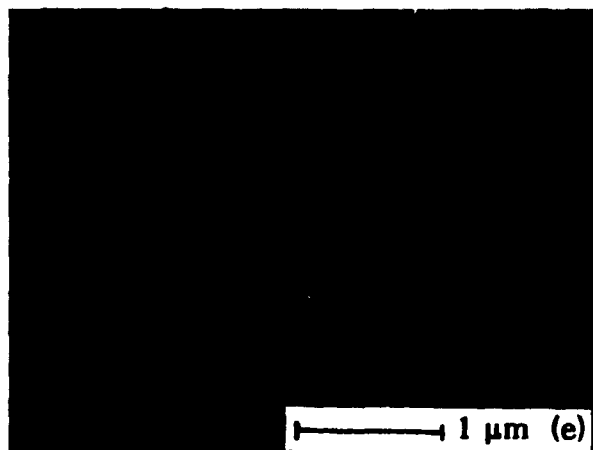


Figure 5.11: Micrographs of AlN powders produced using (e) T40X (θ - Al_2O_3) and (f) SOL-P3 (γ - Al_2O_3) with cane sugar as a carbon source at 1600 °C for five hours

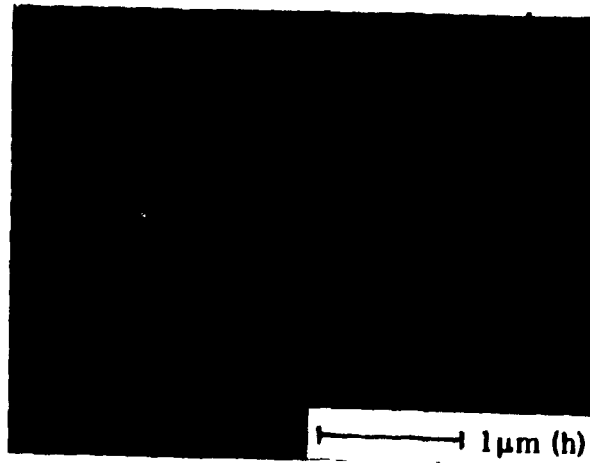
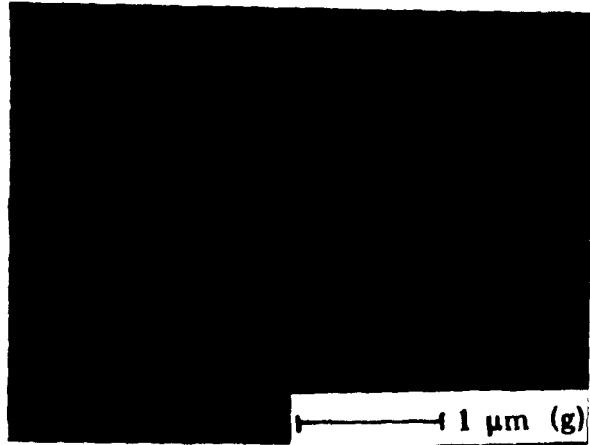


Figure 5.11: Micrographs of commercial AlN powders (g) Tokuyama Soda grade F and (h) Starck grade C

0.053 μm AlN powder and A16SG $\alpha\text{-Al}_2\text{O}_3$ (0.4 μm) produced 0.54 μm AlN powder. This aspect, however, also depends on the nature and morphology of the Al_2O_3 particles; if they are strongly agglomerated and not easily broken up by milling, they do not reflect their original particle size after nitridation (as discussed in section 5.4). This was seen from the results for the AlN produced from SOL P3 (see above). Therefore, it is concluded that the particle size of AlN is strongly dependent on not only the particle size of starting material, but also whether the starting material is agglomerated. The latter depends on the ability to break up the agglomerates and disperse them during precursor preparation.

Figure 5.11 (h) shows the morphology of Starck C AlN powder, which is produced commercially by direct nitridation. This micrograph shows irregular shaped and widely distributed particles and indicates the poor powder quality relative to, in particular, the α alumina-derived powders and the commercial Tokuyama Soda powder. Indeed the quality of the α alumina-derived powders produced in this study are very close to that of the Tokuyama Soda powder (see Figure 5.11 (a), (b) and (g)).

5.6 REACTION MECHANISM AND NITRIDATION

5.6.1 Effect of Carbon Source

Figure 5.12 shows the morphology of AlN powders which were produced using either carbon black or cane sugar as a carbon source with A16SG Al_2O_3 . The AlN produced using carbon black (Figure 5.12(b)) had a very wide particle size distribution and large average particle size. On the other hand, AlN produced using

cane sugar (Figure 5.12 (a)) had a much smaller particle size and a significantly narrower particle size distribution. Therefore, it is believed that the carbon source has a strong effect on the conversion to AlN and the morphology of the powder, and may be the result of the mixing efficiency. Improved mixing is possible using cane sugar due to the fact that it dissolves in water and essentially coats the oxide particles upon drying. Hence, due to the more intimate carbon/oxide contact, less excess carbon is required for full conversion of Al_2O_3 to AlN. From Figure 5.12, the improved mixing also reduces the particle size and distribution. The reason for this is again believed to be due to the sugar coating the entire free surface of each Al_2O_3 particle (or agglomerate), thus limiting the contact between them so that after carburization each individual particle is coated with carbon and separated from adjacent ones. This limits the amount of Al_2O_3 sintering which can occur during the early stages of reaction. This is confirmed by Figure 5.12 (a) for A16SG where the particle size of the starting material ($0.4\mu\text{m}$) is comparable to that of the final AlN particle size of $0.5\mu\text{m}$.

However, when carbon black is used (which also tends to strongly agglomerate), it is difficult to coat the entire free surface of each Al_2O_3 particle due to poorer intermixing at the individual particle level. Hence, there is a greater possibility that the Al_2O_3 particles would come into contact and sinter at the early stages of reaction prior to nitridation and become larger particles. Using this argument, it is suggested that the AlN powder produced using cane sugar also tends to have a more equiaxed morphology than the AlN produced using carbon black, i.e.,

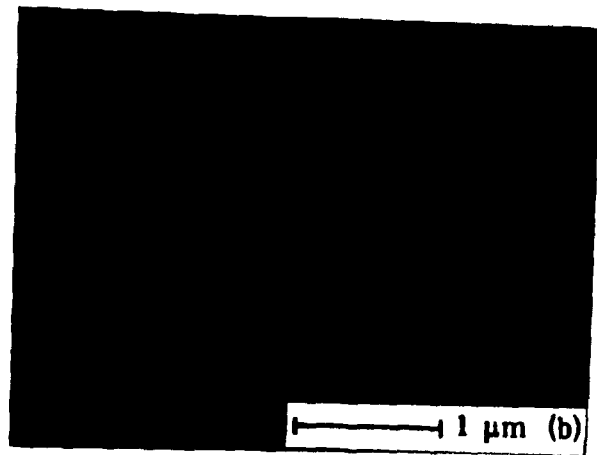
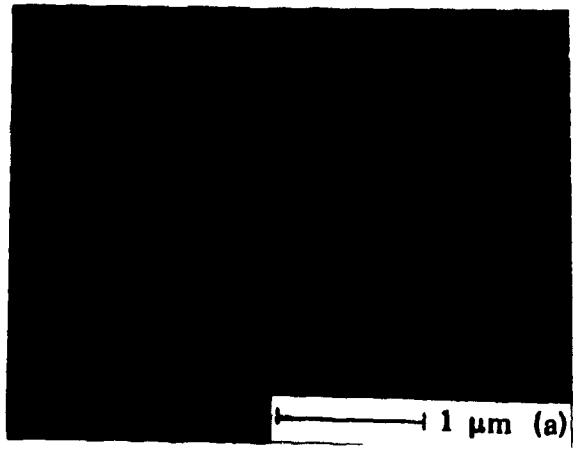


Figure 5.12: Micrographs of AlN powders produced using A16 SG and (a) cane sugar, and (b) carbon black as a carbon source

no sintering or grain growth has occurred in Figure 5.12 (a) whereas a more tabular shaped AlN particles are observed in Figure 5.12 (b), which is typical of coarser aluminas which have undergone grain growth by sintering.

5.6.2 Mechanism of Nitridation

Figure 5.13 shows schematically the model of nitridation sequence when both cane sugar and carbon black are used as a carbon source. As seen in Figure 5.13, C reacts with Al_2O_3 and to form CO gas. This gas diffuses out through the pores in the C coating, during which time N_2 gas diffuses into the pellets to react with the reduced Al_2O_3 forming AlN.

When soluble cane sugar is used as a carbon source (Figure 5.13(a)), it forms a porous C coating after the carburization process and can coat the entire free surface of Al_2O_3 . Thus when sub-micron, regular shaped Al_2O_3 particles are coated, and an excess of N_2 gas is supplied, the reaction may proceed with CO and N_2 gases able to diffuse in and out freely. Therefore, nitridation of each individual particle can occur rapidly leading to a product with the morphology and size similar to that of the starting Al_2O_3 particles.

However, when carbon black is used as a carbon source (Figure 5.13(b)), it will not coat the entire free surface of individual Al_2O_3 particles, thus, the Al_2O_3 particles themselves agglomerate. Therefore, in the early stage of nitriding, sintering and grain growth of the agglomerated Al_2O_3 particles can occur since the reaction temperature is higher than the typical sintering temperature of Al_2O_3 (1400

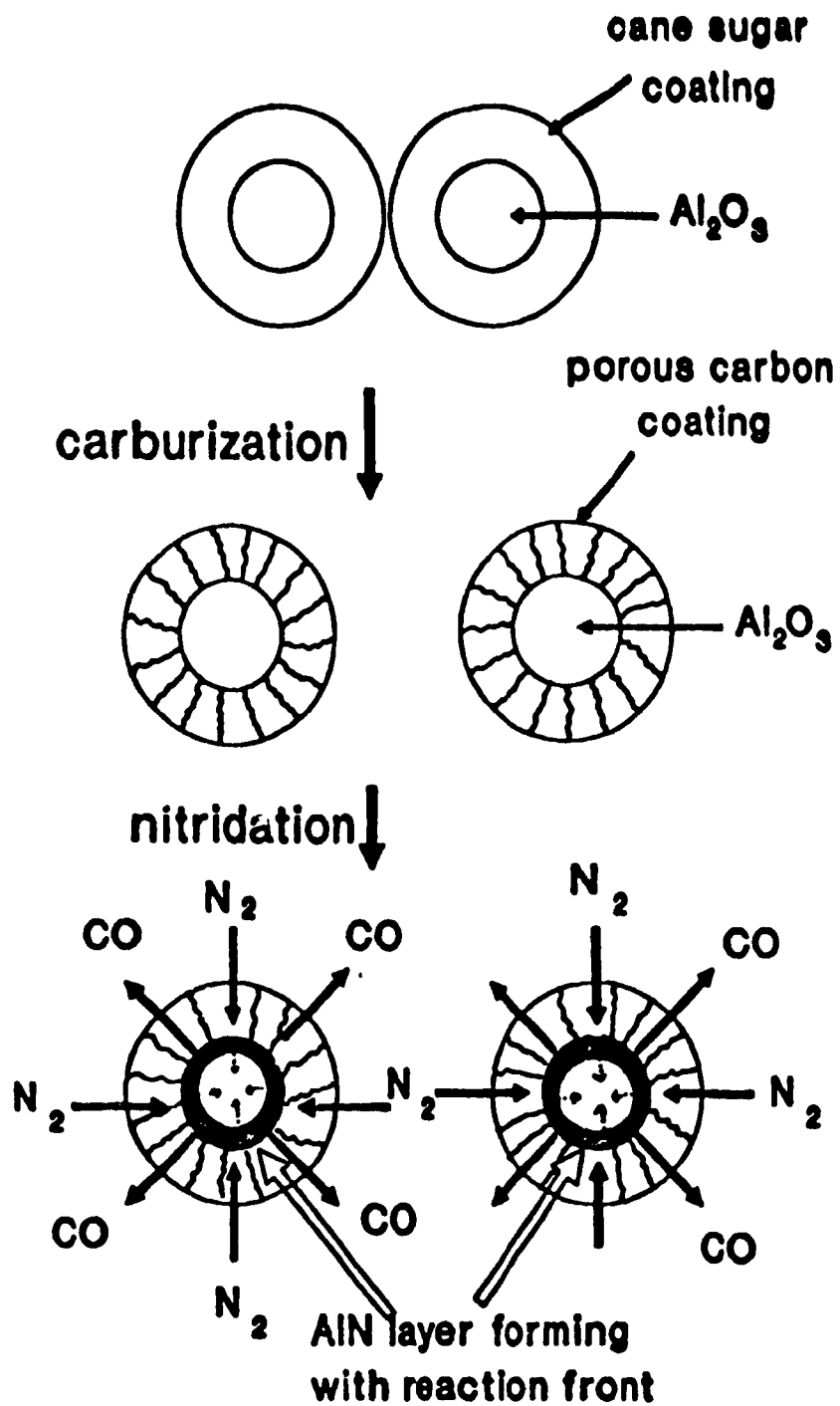


Figure 5.13: (a) The schematic model of the anticipated reaction sequence when cane sugar is used as a carbon source

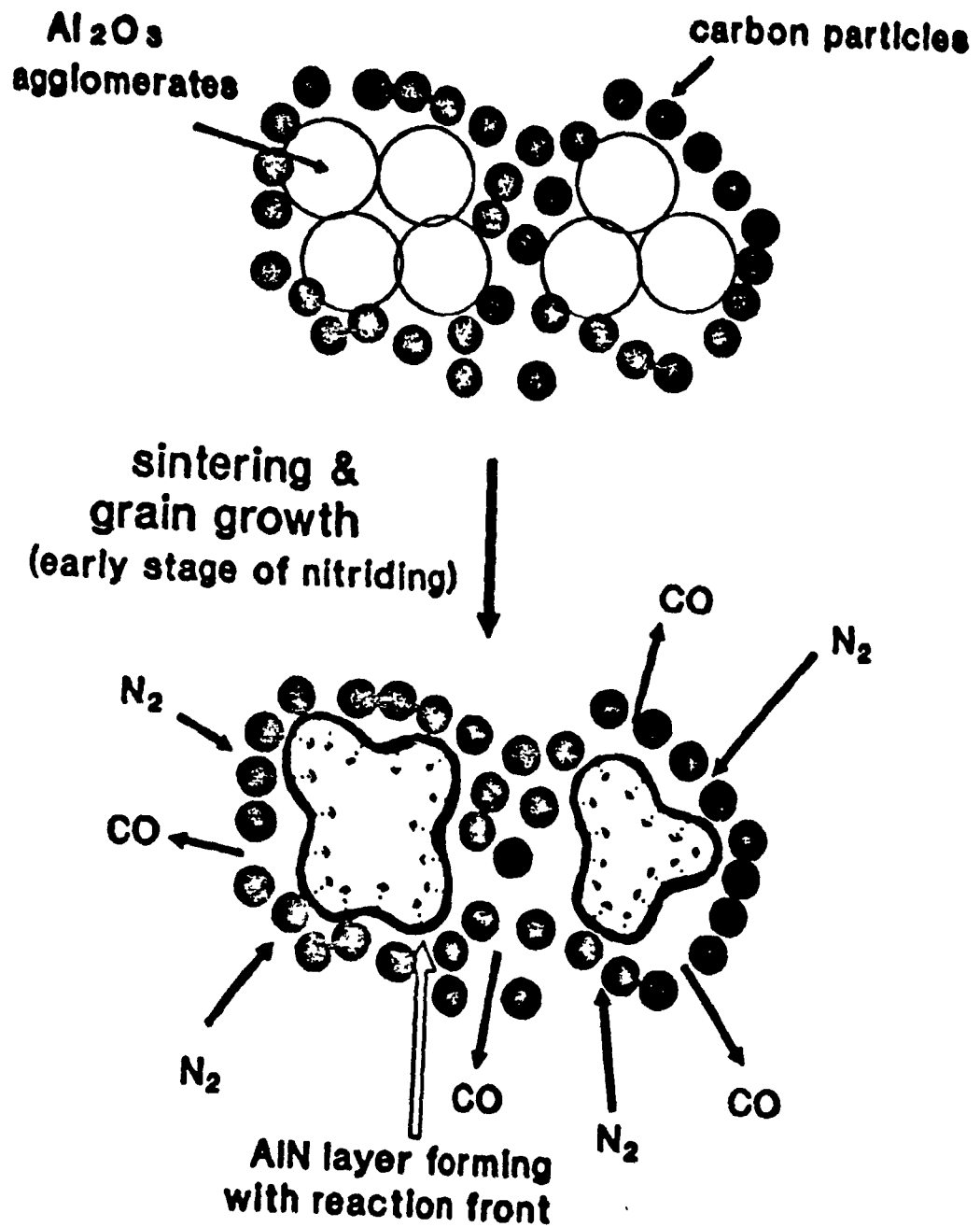


Figure 5.13: (b) The schematic model of the anticipated reaction sequence when carbon black is used as a carbon source

- 1650 °C). Therefore, after nitridation, AlN powders produced using carbon black contain large and irregular shape of particles which do not reflect the original morphology of its starting Al₂O₃ powder.

It is believed that the rate of carbothermal reduction of Al₂O₃ is governed by solid state diffusion. Therefore, the reaction time is dependent on diffusion distances, which for a large sintered agglomerate (such as when carbon black is used) will be greater than for individually coated particles (such as when cane sugar is used). This can be clearly shown in Figures 5.13 which represent the sequence of the solid-state diffusion when (a) cane sugar and (b) carbon black are used. This is supported by the results of the reaction time study discussed in section 5.2, i.e., the Al₂O₃ source having a large particles/agglomerates size requires a longer reaction time to achieve full conversion than finer particle-sized Al₂O₃. In addition, the presence of water in the alumina precursors may provide an additional driving force for improved nitridation kinetics, however, this requires further investigation.

5.7 SINTERING AND THERMAL CONDUCTIVITY

The AlN powders produced using different starting materials, as well as two commercial AlN powders, were sintered with 4 wt.% of Y₂O₃ at 1850 °C for 100 minutes. This sintering condition was suggested by Virkar et al.⁷ to be the optimum for Tokuyama Soda AlN, which was also used as a base-line comparison in this work. The results of sintering of these powders are given in Table 5.4. The cation impurity levels, which were analyzed by X-ray fluorescence method, of the AlN powders used

in this section of experiment did not show significant difference from those of the commercial powders.

The AlN pellets derived from HPA-0.5 and Bacosol 3C, with their lower oxygen and carbon contents (<2 %, <0.2 %), showed the highest thermal conductivities (> 80 W/mK) and fired densities ($\sim 3.30 \text{ g/cm}^3$) of all the powders. The pellets using Bacosol 3A and Alcoa A16SG derived AlNs, with their lower fired densities clearly show very low thermal conductivities (< 55 W/mK) as might be expected for a relatively porous material. The pellet from the Tokuyama Soda displayed higher thermal conductivity than the highest value obtained from the powders produced during this study but slightly lower than the literature thermal conductivity value of 130 - 160 W/mK^{7,23}. The thermal conductivity of Starck C was not a particularly high value, but it is as high as the thermal conductivity value of HPA-0.5, which has better powder morphology and is the highest value among the powders produced in this study. The difference in thermal conductivity values between the experimental results and the literature could be caused by several factors: (1) the O₂ content might vary from batch to batch of powder or the O₂ content might have increased due to moisture pick up during handling, in the case of the commercial powders (2) other metallic impurities might have been introduced during the pellet preparation process, and (3) sintering conditions, such as powder compacting pressure, sintering temperature, atmosphere in the furnace, particle size of Y₂O₃, etc, would not be exactly the same as those used in the literature, (4) the specific heat value of AlN used for the thermal conductivity calculation in this

Table 5.4: The fired density, chemical analysis, and thermal conductivity values of sintered pellets

Starting Material	Density (g/cm ³)	O ₂ Content (%)	C Content (%)	Thermal Conductivity (W/mK)
Alcoa A16SG	3.23	1.52	0.16	52.09
HPA-0.5	3.30	1.13	0.18	88.70
Bacosol 3C	3.30	1.40	0.10	81.89
Bacosol 3A	3.28	1.63	0.13	52.65
Commercial AlN				
Starck C	3.29	2.37	0.26	89.16
Tokuyama Soda	3.28	1.25	0.21	128.50

study might be different from those used in the literatures; i.e. in this study, the specific heat value used was 0.738 W·sec./g·K, which was obtained from the technical bulletin of Keramont Corporation.

The factors controlling the sintering behaviour and their effect on the thermal conductivity are not well understood. However, from the results shown in Table 5.4 and published in the literature,²³ it is evident that there is a strong correlation between the characteristics of the AlN powder used and the sintering cycle necessary to achieve the highest thermal conductivity. These aspects will be explained in future work, particularly with respect to the AlN powder properties.

CHAPTER 6. CONCLUSIONS AND FUTURE WORK

6.1 CONCLUSIONS

Sub-micron particle size, high purity AlN can be produced using the carbothermal reduction process through careful selection of starting materials and control of the processing parameters, such as the choice of a carbon and Al₂O₃ source, reaction temperature and reaction time.

1) The use of cane sugar as a carbon source enables the amount of carbon to be reduced to the close-to-stoichiometric ratio of Al₂O₃ : C = 1 : 3.2. In addition, the use of cane sugar as a carbon source produced equiaxed, sub-micron size particles of AlN due to the superior intermixing of an Al₂O₃ source with the carburized sugar. However, significantly higher amounts of carbon were required to achieve full conversion of AlN when carbon black was used, i.e. Al₂O₃ : C > 1 : 6 and poorer powder quality is obtained due to relatively poor intermixing and agglomeration effects.

When cane sugar was used as a carbon source, the particle size of the reactivity of Al₂O₃ source did not strongly affect the conversion rate of Al₂O₃ to AlN, while the use of carbon black showed marked differences in the conversion rate between the use of boehmite (Bacosol 3C) and Al₂O₃ (Alcoa A16, SG), i.e., the conversion rate of Bacosol 3C was higher than that of A16 SG due to its higher reactivity and finer particle size.

2) The full conversion of Al_2O_3 to AlN was achieved at a reaction temperature of $1600\text{ }^\circ\text{C}$ with the ratio $1 : 3.5$ of $\text{Al}_2\text{O}_3 : \text{C}$ using cane sugar as a carbon source. The activation energy calculated for Bacosol 3C and A16SG were 365.6 kJ/mole and 257.4 kJ/mole , respectively, and the following expressions were derived with the reaction constants determined for both materials:

$$K_{\text{B3C}} = 4.1 \times 10^{-7} \exp(-356.6 \text{ kJ/RT})$$

$$K_{\text{A16SG}} = 1.4 \times 10^{-6} \exp(-257.6 \text{ kJ/RT}).$$

These values are comparable to those determined for the O_2 lattice diffusion in Al_2O_3 ($238 - 636\text{ kJ/mole}$) indicating that the experimental values are consistent with solid state diffusion of these species occurring as the rate determining step the carbothermal reduction of Al_2O_3 to AlN .

When the reaction temperature was higher than $1600\text{ }^\circ\text{C}$, more agglomeration of AlN particles was observed due to partial sintering of AlN . In order to achieve full conversion below $1600\text{ }^\circ\text{C}$, a greater excess of carbon was required.

3) The minimum reaction time for full conversion at $1600\text{ }^\circ\text{C}$ was dependent upon the use of the Al_2O_3 source, i.e. a shorter reaction time was needed for a finer and more reactive Al_2O_3 source, whilst a longer reaction time was needed for a coarser and less reactive Al_2O_3 source. Again, the aspect of conversion rate below the minimum reaction time showed differences depending on the particle size and reactivity of Al_2O_3 source used. Furthermore, the degree of agglomeration of particles also affected the conversion rate, i.e. even though an Al_2O_3 source had

fine particles, when its degree of agglomeration was high, the reaction rate became low (e.g. in the case of Bacosol 3C).

4) The particle sizes and the agglomerate size of AlN powders did not significantly increase with increasing reaction time for a maximum of ≤ 5 hour at 1600 °C. It was shown that agglomeration mainly occurred in the precursor state due to sintering of Al₂O₃ particles in the early stages of reaction prior to nitridation. The morphology of AlN powder was strongly dependent upon the morphology of the Al₂O₃ source used when cane sugar was a carbon source: fine particle-sized Al₂O₃ source produced fine particle-sized AlN powder and conversely, coarse Al₂O₃ produced a coarse AlN powder. However, when the particle size of Al₂O₃ source was extremely small ($< 0.05 \mu\text{m}$), it tended to strongly agglomerate and was difficult to deagglomerate (Sol-P3), and this was directly reflected in the morphology of AlN powder produced.

5) The carbothermal nitridation reaction is considered to be mainly a solid state reaction. It is believed that this reaction mechanism occurs by diffusion of CO and N₂ gas. Therefore, the rate of the diffusion depends on diffusion distance, which for a large sintered agglomerate (when carbon black was used) will be greater than for individually coated particles (as for cane sugar).

6.2 SUGGESTED FUTURE WORK

1) The use of cane sugar has shown many advantages in the morphology of AlN powder and the ratio of Al_2O_3 : C, however, the carburization of cane sugar (pyrolysis) processes over a period of 3 - 4 days adds to the processing time. It is suggested that more efficient method of the carburization of cane sugar should be investigated including to control the exact amount of carbon yield from cane sugar.

2) This work has shown that ball milling for 18 hours leads to satisfactory intermixing between cane sugar and Al_2O_3 source. However, this mixing method was not able to break down some agglomeration of the Al_2O_3 particles, Therefore, it is suggested that the effect of milling time and other mixing methods be investigated.

3) The reaction kinetics and mechanism, as well as the effect of N_2 gas flow-rate on conversion should be studied further.

4) In this study some AlN powders were sintered and gave values close to the theoretical density. However, the thermal conductivities of these materials were less than optimum. Therefore, the sintering behaviour of AlN powder should be studied in more detailed (e.g. sintering temperature and time, and the effect of sintering additive) so as to improve the thermal conductivity and better understand the relationship between sintered microstructure and thermal conductivity.

REFERENCES

- 1 R. Bachelard, P. Joubert, "Aluminum Nitride by Carbothermal Reduction J. Mat. Sci. Eng., A109 (1989), 247
- 2 A. Kurokawa, K. Utsumi, H. Takamizawa, T. Kamata, S. Noguchi, "AlN Substrates with High Thermal Conductivity", IEEE Tran. Comp. Hib. Manuf. Tech., CHMT-8(2) (1985), 247
3. L.M. Sheppard, "Aluminum Nitride: A Versatile but Challenging Material", Am. Ceram. Soc. Bull., 69 (1990), 1801
- 4 N. Kuramoto, H. Taniguchi, I. Aso, "Development of Translucent Aluminum Nitride Ceramics", Am. Ceram. Soc. Bull. 68 (1989), 886
- 5 L.M. Sheppard, Ed., "Aluminum Nitride: A Versatile but Challenging Material", Am. Ceram. Soc. Bull., 69 (1990), 1807
- 6 N. Kuramoto, H. Taniguchi, U.S. Patent No. 4618592 (1986)
- 7 A.V. Virkar, T.B. Jackson, R.A. Culter, "Thermodynamic and Kinetic Effect of Oxygen Removal on the Thermal Conductivity of Aluminum Nitride", J. Am. Ceram. Soc., 72(11) (1989), 2031
- 8 M.P. Borom, G.A. Slack, J.W. Szymaszek, "Thermal Conductivity of Commercial Aluminum Nitride" Am. Ceram. Soc. Bull., 51(11) (1972), 852
- 9 G.A. Slack, T.F. McNelly, "Growth of High Purity AlN Crystals", J.Crys. Grow., 34 (1976), 263

- 10 K.M. Taylor, C. Lenie, "Some Properties of Aluminum Nitride", J. ElectChem. Soc., 107(4) (1960), 308
- 11 R. Chanchani, "Processability of Thin-Film, Fine-Line Pattern on Aluminum Nitride Substrates", IEEE Trans. Comp. Hib. Manuf. Tsch., CHMT-11(4) (1988), 427
- 12 I. Kimura, N. Hotta, H. Nuki, N. Saito, S. Yasukawa, "Particulate Characteristics and Deposition Features of Fine AlN Powder Synthesized by Vapour-Phase Reaction", J. Mat. Sci., 24 (1989), 4076
- 13 M. David, S.V. Babu, D.H. Rasmussen, "RF Plasma Synthesis of Amorphous AlN Powder and Films", AIChE J, 36(6) (1990), 871
- 14 K. Shanker, S. Grenier, R.A.L. Drew, "Synthesis of Nitride Ceramics by Carbothermal Reduction", Proc. 3rd Intl. Conf. on Ceramic Processing Science, 1990, San Diego, CA.
- 15 A. Tsugar, H. Inoue, M. Kasori, K. Shinozaki, "Raw Material Effect on AlN Powder Synthesis from Al₂O₃ Carbothermal Reduction", J. Mat. Sci., 25 (1990), 2359
- 16 W.L. Li, L.P. Huang, G. Kuang, S.H. Tan, S.R. Fwu, T.S. Yen, "Preperation of Some High Purity Ultrafine Non-oxide Powder", Ed. P.Vincenzini, Elsevier,(1983), 403
- 17 L.D. Silverman, "Carbothermal Synthesis of Aluminum Nitride" Adv. Ceram. Mat., 3(4) (1988), 418
- 18 B.I. Lee, M.A. Einasrud, "Low-Temperature Synthesis of Aluminum Nitride via Liquid-Liquid Mix Carbothermal Reduction", J. Mat. Sci. Letters, 9 (1990), 1398
- 19 W. Rafaniello, M.S. Paquette, T.D. Rey, "Examination of Commercial AlN Powders", The Dow Chem. Comp.

- 20 M. Mitomo, Y. Yoshioka, "Preparation of Si_3N_4 and AlN Powders from Alkoxide-Derived Oxide by Carbothermal Reduction and Nitridation", *Adv. Ceram. Mat.*, 2(3A) (1987), 253
- 21 H. Buhr, G. Muller, H. Wiggers, "Phase Composition Content and Thermal Conductivity of $\text{AlN}(\text{Y}_2\text{O}_3)$ Ceramics", *J. Am. Soc.*, 74(4) (1991), 718
- 22 N.S. VanDamme, S.M. Richard, S.R. Winzer, "Liquid-Phase Sintering of Aluminum Nitride by Europium Oxide Additives", *J. Am. Ceram. Soc.*, 72(8) (1989), 1409
- 23 T.B. Troczynski, P.S. Nicholson, "Effect of Additives on the Pressureless Sintering of Aluminum Nitride between 1500 °C and 1800 °C", *J. Am. Ceram. Soc.*, 72(8) (1989), 1488
- 24 S.J.P. Durham, Ph.D Thesis, "Carbothermal Reduction of Silica to Silicon Nitride Powder", McGill University, (1989), 44
- 25 S. Brunauer, P. Emmett, E. Teller, *J. Am. Chem.*, 60, (1938)
- 26 E. Dorre, H. Hubner, "Alumina: Processing, Properties, and Applications", Ed. B. Ilschner, N.J. Grant, Springer-Verlag Berlin, Germany, 1984
- 27 D.H.P. Hasselman, G.A. Merkel, "Specimen Size Effect of the Thermal Diffusivity/Conductivity of Aluminum Nitride", *J. Am. Ceram. Soc.*, 72(6) (1989), 967
- 28 C.W. Bale, A.D. Pelton, W.T. Thompson, F*A*C*T-Facility for the Analysis of Chemical Thermodynamics Guide to Operators, McGill University/Ecole Polytechnique, Montreal, Canada, (1985)

29 H.H. Kellogg, S.K. Basru, Trans. Metall. Soc. AIME. 218 (1960), 70

30 C.W. Bale, A.D. Pelton, W.T. Thompson, Canadian Metallurgical Quarterly, 25 (1989), 67, 72-74

APPENDICES

APPENDIX I:

QUANTITATIVE X-RAY DIFFRACTION ANALYSIS

The amount of converted AlN in the carbothermally synthesized powder was determined by X-ray diffraction. To generate a calibration plot, mixtures of Al₂O₃ (Alcoa A16SG) and AlN (Tokuyama Soda, F) were used. Known ratios (from 0 to 100 wt% AlN) were mixed in isoprapanol and rapidly dried in a microwave oven, and then exposed to filtered CuK α radiation, using a Philips X-ray diffractometer (APD 1700). The intensity of the 100 % (100) hkl plane for AlN, shown at 2 θ , of 33.2 ° and that of the 100 % (104) hkl plane for Al₂O₃, shown at 2 θ , of 35.2 ° were used to plot the calibration curve. Since the Al₂O₃ diffraction peak intensity is greater than that of AlN for comparable compositions, the analysis is more sensitive to small amounts of Al₂O₃. The AlN powders produced were scanned over 2 θ of 30 - 40 ° with a scanning rate of 1 °/sec. This calibration curve is shown in Figure A-I, and the calculation determining the amount of unreacted Al₂O₃ is based on the heights of intensity peaks chosen above:

$$W_{Al_2O_3} = I_{Al_2O_3} / (I_{Al_2O_3} + I_{AlN}) \quad (I.1)$$

The principal errors of this calculation can be caused by the measurement of the peak height and the minimum peak detectable above the background noise.

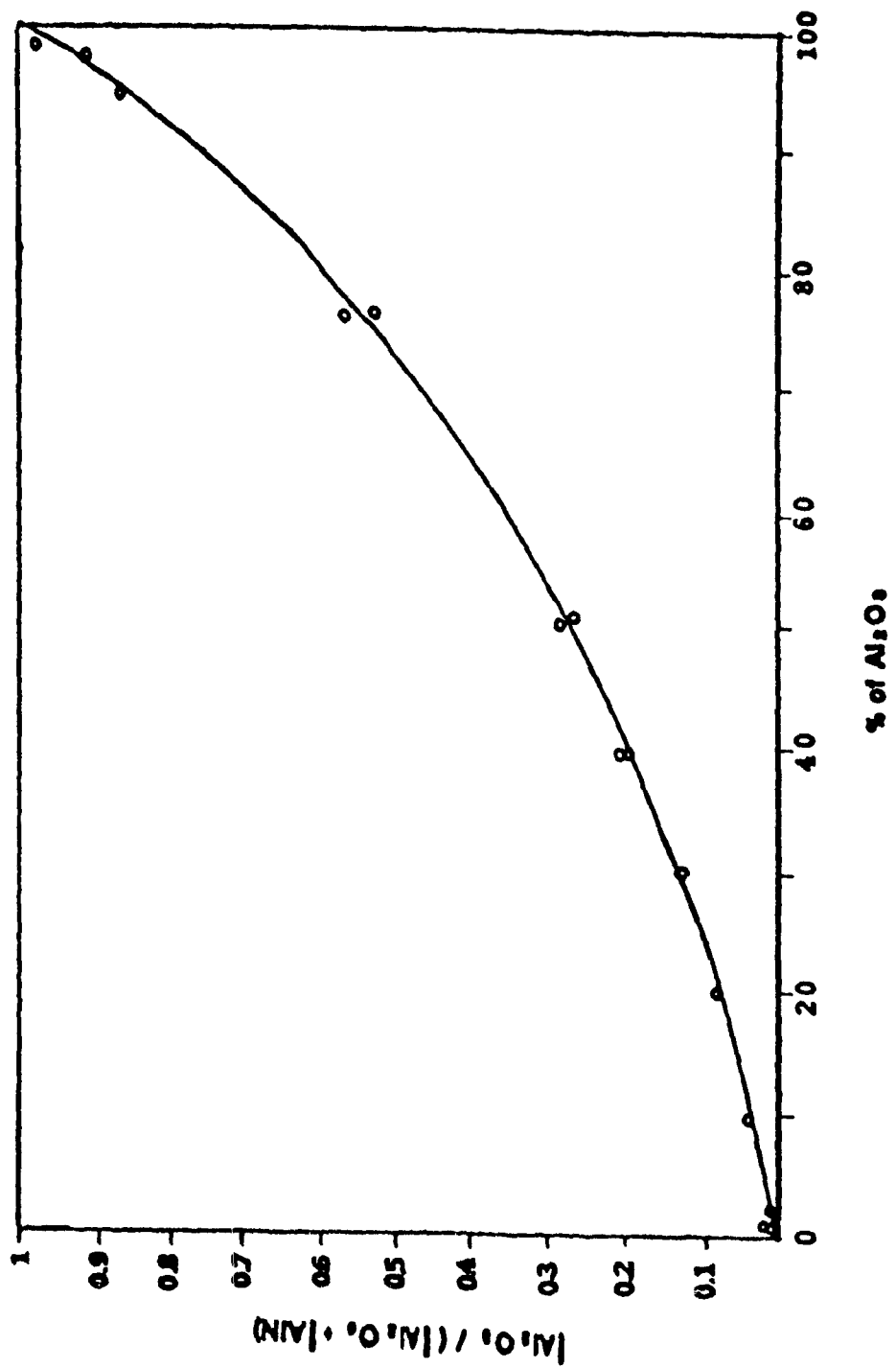


Figure 1: XRD calibration curve for quantitation of unreacted Al₂O₃ in AlN powder

APPENDIX II:

THERMODYNAMIC DATA OF THE Al-N-O-C SYSTEM

APPENDIX II.1 THERMODYNAMIC CALCULATIONS

RESULTS OF EQUILB PROGRAM

Table II.1: Partial pressures of N₂, CO, CO₂, Al₂O₂ and O₂ for the equation of Al₂O₃ + 3C + <A>N₂ at 1873 K

<A> (mol)	P(N ₂) (atm)	P(CO) (atm)	P(CO ₂) (atm)	P(Al ₂ O ₂) (atm)	P(O ₂) (atm)
1	0.562	0.438	0.928E-5	0.969E-12	0.837E-16
41	0.930	0.698E-1	0.344E-6	0.318E-13	0.454E-17
81	0.964	0.361E-1	0.141E-6	0.190E-13	0.282E-17
121	0.976	0.244E-1	0.812E-7	0.138E-13	0.207E-17
161	0.982	0.184E-1	0.545E-7	0.108E-15	0.163E-17
201	0.985	0.148E-1	0.409E-7	0.941E-14	0.143E-17

Table II.2: Partial pressures of N₂, CO, CO₂, Al₂O₂ and O₂ for the equation of Al₂O₃ + 3C + 106.5N₂, at several temperatures

Temp. (K)	P(N ₂) (atm)	P(CO) (atm)	P(CO ₂) (atm)	P(Al ₂ O ₂) (atm)	P(O ₂) (atm)
1673	0.972	0.277E-1	0.129E-6	0.787E-16	0.551E-19
1723	0.972	0.277E-1	0.109E-6	0.275E-15	0.126E-18
1773	0.972	0.277E-1	0.107E-6	0.121E-14	0.372E-18
1823	0.972	0.277E-1	0.105E-6	0.475E-14	0.101E-17
1873	0.972	0.277E-1	0.990E-7	0.160E-13	0.239E-17
1923	0.972	0.277E-1	0.851E-7	0.417E-13	0.448E-17

Table II.3: Partial pressures of N₂, CO, CO₂, Al₂O₂ and O₂ for the equation of Al₂O₃ + 6C + <A>N₂, at 1873 K

<A> (mol)	P(N ₂) (atm)	P(CO) (atm)	P(CO ₂) (atm)	P(Al ₂ O ₂) (atm)	P(O ₂) (atm)
5	0.571	0.429	0.889E-5	0.912E-12	0.801E-16
10	0.750	0.250	0.302E-5	0.237E-12	0.273E-16
15	0.824	0.176	0.151E-5	0.107E-12	0.136E-16
20	0.864	0.136	0.900E-6	0.611E-13	0.811E-17
25	0.900	0.111	0.597E-6	0.394E-13	0.539E-17
30	0.906	0.937E-1	0.425E-6	0.275E-13	0.383E-17
35	0.919	0.811E-1	0.318E-6	0.203E-13	0.287E-17
45	0.936	0.638E-1	0.197E-6	0.124E-13	0.178E-17
85	0.966	0.345E-1	0.575E-7	0.350E-14	0.519E-18
125	0.976	0.236E-1	0.270E-7	0.162E-14	0.243E-18
165	0.982	0.180E-1	0.156E-7	0.933E-15	0.141E-18

Table II.4: Partial pressures of N₂, CO, CO₂, Al₂O₂ and O₂ for the equation of Al₂O₃ + 6C + 106.5N₂, at several temperatures

Temp. (K)	P(N ₂) (atm)	P(CO) (atm)	P(CO ₂) (atm)	P(Al ₂ O ₂) (atm)	P(O ₂) (atm)
1673	0.972	0.277E-1	0.129E-6	0.787E-16	0.551E-19
1723	0.972	0.277E-1	0.914E-7	0.196E-15	0.897E-19
1773	0.972	0.277E-1	0.664E-7	0.461E-15	0.142E-18
1823	0.972	0.2771E-1	0.492E-7	0.104E-14	0.220E-18
1873	0.972	0.2771E-1	0.370E-7	0.223E-14	0.334E-18
1923	0.972	0.2771E-1	0.283E-7	0.462E-14	0.495E-18

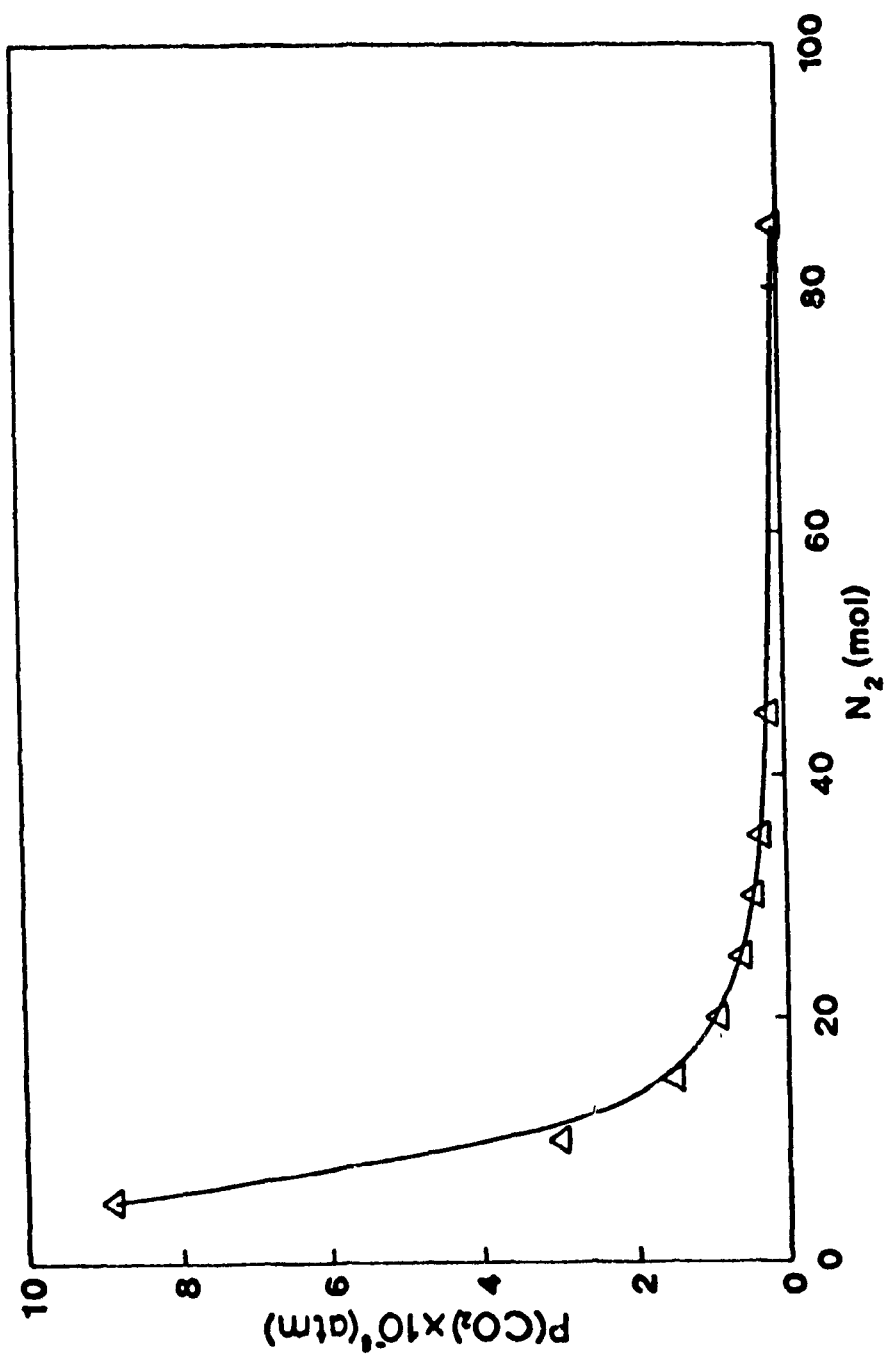


Figure II.1: Partial pressure of CO₂ vs. amount of N₂ gas introduced at 1600 °C (Al₂O₃ : C = 1 : 6)

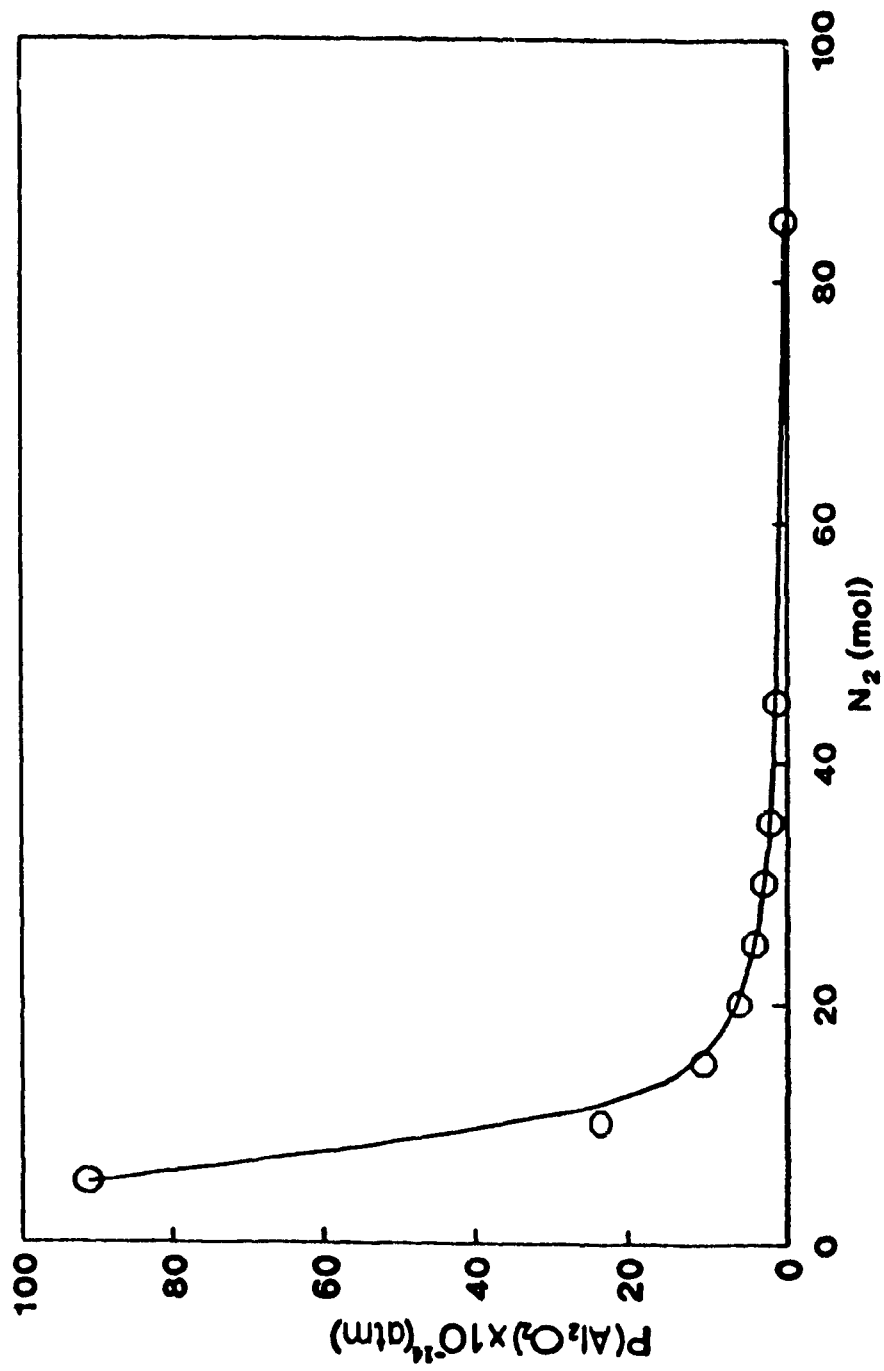


Figure II.2: Partial pressure of Al_2O_2 vs. amount of N_2 introduced at $1600\text{ }^\circ\text{C}$ ($\text{Al}_2\text{O}_3 : \text{C} = 1 : 6$)

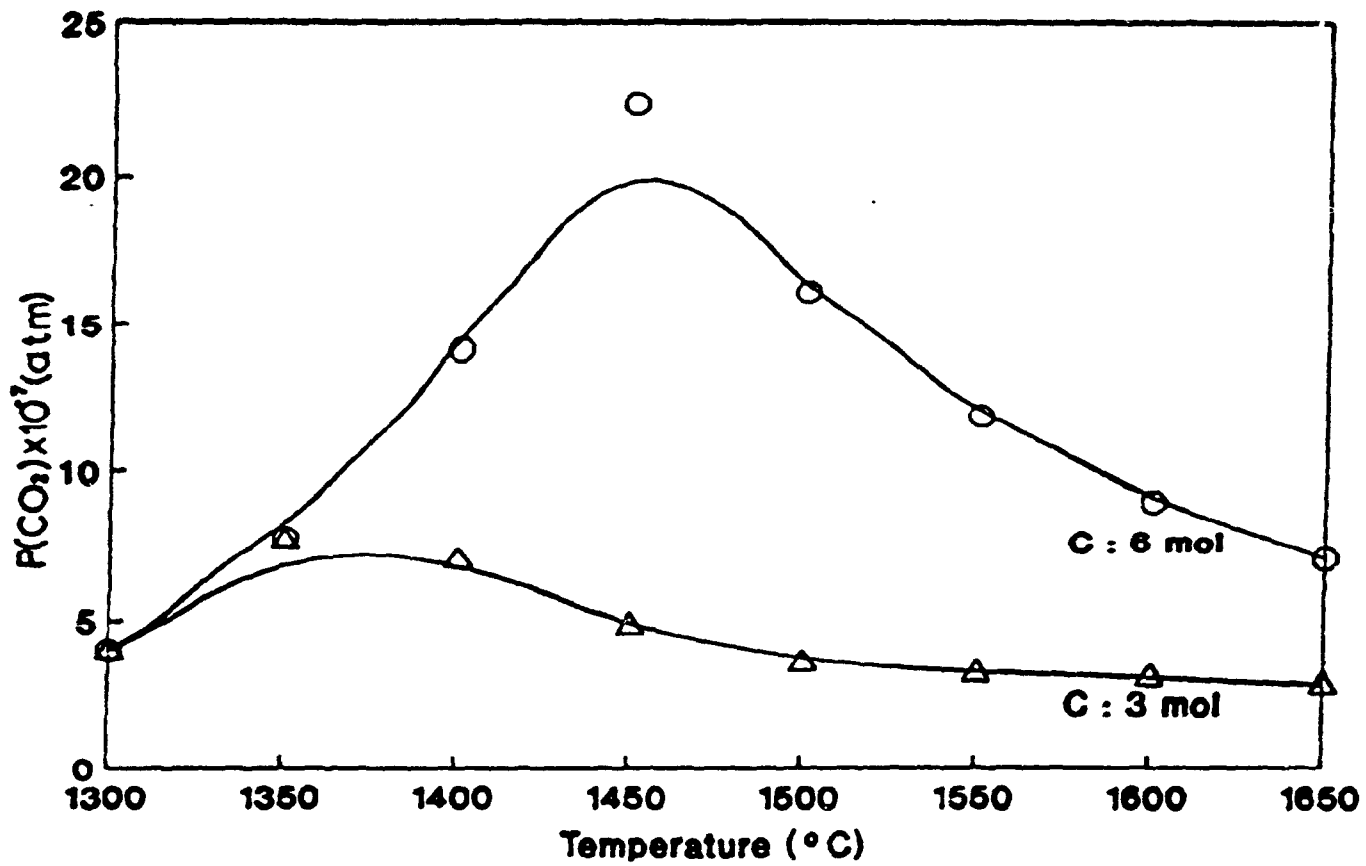


Figure II.3: Partial pressure of CO₂ as a function of temperature

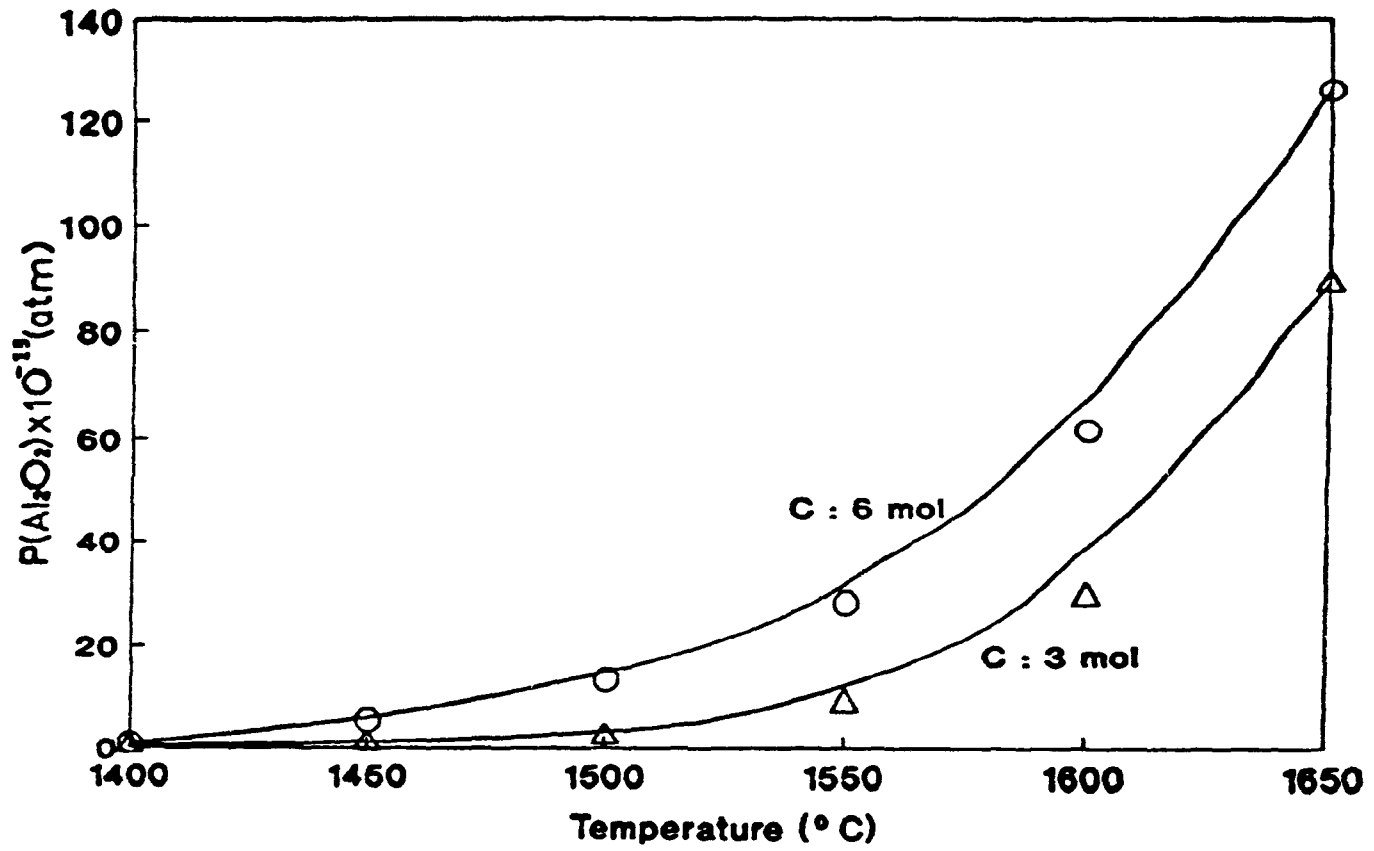


Figure II.4: Partial pressure of Al_2O_2 as a function of temperature

PAGINATION ERROP.

ERREUR DE PAGINATION.

TEXT COMPLETE.

LE TEXTE EST COMPLET.

NATIONAL LIBRARY OF CANADA.

BIBLIOTHEQUE NATIONALE DU CANADA.

CANADIAN THESES SERVICE.

SERVICE DES THESES CANADIENNES.

INSPECT PROGRAM

FORMULA: AlN
 NAME: ALUMINUM MONONITRIDE
 FORMULA WEIGHT: 40.988

PHASE NAME CP RANGE (K)

S1 SOLID 298.0 - 600.0
 S1 SOLID 600.0 - 1000.0
 S1 SOLID 1000.0 - 2000.0

$$CP = A + 1.0E-3*B*T(K) + 1.0E5*C*T(K)**-2 + 1.0E-6*D*T(K)**2$$

PHASE	DH(298) (KJ)	S(298) (J /K)	DENSITY (g/cm ³)	A -----	B (J /K)-----	C	D
S1	-317.984	20.150	3.260	32.267	22.686	-7.904	0.0
S1	-317.423	21.779	3.260	50.216	1.172	-26.054	0.0
S1	-319.052	17.984	3.260	50.141	0.389	-17.397	0.0

REFERENCE:

"THERMOCHEMICAL PROPERTIES OF INORGANIC SUBSTANCES",
 I. BARIN, O. KNACKE, AND O. KUBASCHEWSKI,
 SPRINGER-VERLAG, BERLIN, 1977.

FORMULA: Al₂O₃

NAME: ALUMINUM OXIDE

FORMULA WEIGHT: 101.961

PHASE NAME CP RANGE (K)

S1 CORUNDUM 298.0 - 800.0
 S1 CORUNDUM 800.0 - 2327.0 D H TRANS (2327.00 K) = 118.407 (K J)
 L1 LIQUID 2327.0 - 3500.0

$$CP = A + 1.0E-3*B*T(K) + 1.0E5*C*T(K)**-2 + 1.0E-6*D*T(K)**2$$

```
*****
PHASE  DH(298) S(298) DENSITY  A    B    C    D
      (K J)  (J /K) (g/cm3)  -----( J /K)-----
*****
```

PHASE	DH(298) (K J)	S(298) (J /K)	DENSITY (g/cm ³)	A	B	C	D
S1	-1675.274	50.936	3.970	103.851	26.267	-29.091	0.0
S1	-1674.876	52.392	3.970	120.516	9.192	-48.367	0.0
L1	-1595.529	45.144	3.970	144.863	0.0	0.0	0.0

REFERENCE:

"THERMOCHEMICAL PROPERTIES OF INORGANIC SUBSTANCES",
I. BARIN, O. KNACKE, AND O. KUBASCHEWSKI,
SPRINGER-VERLAG, BERLIN, 1977.

FORMULA: Al₂O₂
NAME: DIMERIC ALUMINUM MONOXIDE
FORMULA WEIGHT: 85.962

PHASE	NAME	CP RANGE (K)
G1	GAS	298.0 - 2000.0

$$CP = A + 1.0E-3*B*T(K) + 1.0E5*C*T(K)**-2 + 1.0E-6*D*T(K)**2$$

```
*****
PHASE  DH(298) S(298) DENSITY  A    B    C    D
      (K J)  (J /K) (G/CM**3)  -----( J /K)-----
*****
```

PHASE	DH(298) (K J)	S(298) (J /K)	DENSITY (G/CM**3)	A	B	C	D
G1	-405.848	266.521	IDEAL	63.660	21.443	-15.736	-6.234

REFERENCE:

"THERMOCHEMICAL PROPERTIES OF INORGANIC SUBSTANCES",
I. BARIN, O. KNACKE, AND O. KUBASCHEWSKI,
SPRINGER-VERLAG, BERLIN, 1977.

FORMULA: AIC
 NAME: ALUMINIUM CARBIDE
 FORMULA WEIGHT: 38.993

PHASE NAME CP RANGE (K)

G1 GAS 298.0 - 2000.0
 G1 GAS 2000.0 - 6000.0

$$CP = A + 1.0E-3*B*T(K) + 1.0E5*C*T(K)**-2 + 1.0E-6*D*T(K)**2$$

```
*****
PHASE  DH(298) S(298) DENSITY  A    B    C    D
      (K J) ( J/K) (G/CM**3) -----( J/K)-----
*****
G1     689.523  223.342  IDEAL  35.363  2.552  -3.452  -0.561
G1     686.774  217.813  IDEAL  36.936  0.536   5.406   0.0
```

REFERENCE:

"JANAF THERMOCHEMICAL TABLES",
 D.R. STULL AND H. PROPHET,
 U.S. DEPARTMENT OF COMMERCE, WASHINGTON, 1977.

FORMULA: Al₄C₃
 NAME: TETRAALUMINUM TRICARBIDE
 FORMULA WEIGHT: 143.959

PHASE NAME CP RANGE (K)

S1 SOLID 298.0 - 1800.0

$$CP = A + 1.0E-3*B*T(K) + 1.0E5*C*T(K)**-2 + 1.0E-6*D*T(K)**2$$

```
*****
PHASE  DH(298) S(298) DENSITY  A    B    C    D
      (K J) ( J/K) (G/CM**3) -----( J/K)-----
*****
S1     -207.275  104.600  2.360  154.691  28.727  -41.940  0.0
```

REFERENCE:

"THERMOCHEMICAL PROPERTIES OF INORGANIC SUBSTANCES",
I. BARIN, O. KNACKE, AND O. KUBASCHEWSKI,
SPRINGER-VERLAG, BERLIN, 1977.

FORMULA: N₂
NAME: NITROGEN
FORMULA WEIGHT: 28.013

PHASE NAME CP RANGE (K)

G1 GAS 298.0 - 2500.0
AQ AQUEOUS 298.0 - 523.0

$$CP = A + 1.0E-3*B*T(K) + 1.0E5*C*T(K)**-2 + 1.0E-6*D*T(K)**2$$

```
*****
PHASE  DH(298) S(298) DENSITY  A    B    C    D
      (K J) ( J /K) (G/CM**3) -----( J /K)-----
*****
G1     0.0  191.502  IDEAL  27.865  4.268  0.0   0.0
AQ    -10.460  94.977  ----- -742.572 1517.629 487.917  0.0
```

REFERENCE:

"THERMOCHEMICAL PROPERTIES OF INORGANIC SUBSTANCES",
I. BARIN, O. KNACKE, AND O. KUBASCHEWSKI,
SPRINGER-VERLAG, BERLIN, 1977.
(FOR THE NON-AQUEOUS SPECIES)

APPENDED TO:

"HANDBOOK OF THERMOCHEMICAL DATA FOR COMPOUNDS AND AQUEOUS
SPECIES",
H.E. BARNER AND R.V. SCHEUERMAN,
WILEY-INTERSCIENCE, NEW YORK, 1978.
(FOR THE AQUEOUS SPECIES)

FORMULA: O₂
 NAME: OXYGEN
 FORMULA WEIGHT: 31.999

PHASE NAME CP RANGE (K)

G1 GAS 298.0 - 3000.0
 AQ AQUEOUS 298.0 - 573.0

$$CP = A + 1.0E-3*B*T(K) + 1.0E5*C*T(K)**-2 + 1.0E-6*D*T(K)**2$$

PHASE	DH(298) (K J)	S(298) (J /K)	DENSITY (G/CM**3)	A	B	C	D
G1	0.0	205.037	IDEAL	29.957	4.184	-1.674	0.0
AQ	-11.715	110.876	----	162.230	32.125	31.614	0.0

REFERENCE:

"THERMOCHEMICAL PROPERTIES OF INORGANIC SUBSTANCES",
 I. BARIN, O. KNACKE, AND O. KUBASCHEWSKI,
 SPRINGER-VERLAG, BERLIN, 1977.
 (FOR THE NON-AQUEOUS SPECIES)

APPENDED TO:

"HANDBOOK OF THERMOCHEMICAL DATA FOR COMPOUNDS AND AQUEOUS
 SPECIES",
 H.E. BARNER AND R.V. SCHEUERMAN,
 WILEY-INTERSCIENCE, NEW YORK, 1978.
 (FOR THE AQUEOUS SPECIES)

FORMULA: CO
 NAME: CARBON MONOXIDE
 FORMULA WEIGHT: 28.010

PHASE NAME CP RANGE (K)

G1 GAS 298.0 - 2500.0
 AQ AQUEOUS ---- CP UNKNOWN, ASSUMED ZERO

$$CP = A + 1.0E-3*B*T(K) + 1.0E5*C*T(K)**-2 + 1.0E-6*D*T(K)**2$$

```
*****
PHASE  DH(298) S(298) DENSITY  A    B    C    D
      (K J)  ( J/K) (G/CM**3) -----( J/K)-----
*****
G1  -110.541  197.552  IDEAL  28.409  4.100  -0.460  0.0
AQ  -120.959  104.600  -----  0.0
```

REFERENCE:

"SELECTED VALUES OF CHEMICAL THERMODYNAMIC PROPERTIES",
 NATIONAL BUREAU OF STANDARDS SERIES 270,
 D.D. WAGMAN ET AL.,
 U.S. DEPARTMENT OF COMMERCE, WASHINGTON, 1968-1971.

APPENDED TO:

"THERMOCHEMICAL PROPERTIES OF INORGANIC SUBSTANCES",
 I. BARIN, O. KNACKE, AND O. KUBASCHEWSKI,
 SPRINGER-VERLAG, BERLIN, 1977.

FORMULA: CO₂
 NAME: CARBON DIOXIDE
 FORMULA WEIGHT: 44.010

```
PHASE  NAME      CP RANGE (K)

G1  GAS      298.0 - 2500.0
AQ  AQUEOUS   ----      CP UNKNOWN, ASSUMED ZERO
```

$$CP = A + 1.0E-3*B*T(K) + 1.0E5*C*T(K)**-2 + 1.0E-6*D*T(K)**2$$

```
*****
PHASE  DH(298) S(298) DENSITY  A    B    C    D
      (K J)  ( J/K) (G/CM**3) -----( J/K)-----
*****
G1  -393.505  213.660  IDEAL  44.141  9.037  -8.535  0.0
AQ  -413.798  117.570  -----  0.0
```

REFERENCE:

"SELECTED VALUES OF CHEMICAL THERMODYNAMIC PROPERTIES",
 NATIONAL BUREAU OF STANDARDS SERIES 270,

D.D. WAGMAN ET AL.,
U.S. DEPARTMENT OF COMMERCE, WASHINGTON, 1968-1971.
APPENDED TO:
"THERMOCHEMICAL PROPERTIES OF INORGANIC SUBSTANCES",
I. BARIN, O. KNACKE, AND O. KUBASCHEWSKI,
SPRINGER-VERLAG, BERLIN, 1977.

APPENDIX II.2

F*A*C*T SYSTEM

F*A*C*T is a mainframe computer-based system designed to be used for the more commonly encountered thermodynamic calculations. Developed by Bale, Pelton and Thompson²⁷, it has a wide range of capabilities which include the calculation of:

1. Reaction heat balances
2. Isothermal/isobaric property changes (ΔH , ΔG , etc.)
3. Elemental or compound vapour pressures
4. Equilibrium products of complex multi-phase chemical reactions
5. Predominance diagrams
6. Binary, ternary and quaternary phase diagrams.

Each of these functions are quite specific in their own right, the outputs of which can be combined together in order to form the basis for the modelling of chemical reactions and systems.

The facility has a large database of thermodynamic properties for over 5000 elements and compounds that can be accessed by the user in calculations. However, the users may also specify his or her own data in order to assess data from other sources, INSPECT program.

The three most applicable facilities of the program to the present work were the calculation of Gibbs energy changes of reactions (REACT), the calculation of equilibrium products for the Al-N-O-C system (EQUILIB) and the calculation of

predominance diagrams (PREDOM).

The EQUILB program calculates the products of a given set of reactants at specified temperatures and pressures, along with various constraints at equilibrium. This is accomplished by iteratively optimizing the number of moles of the selected products in order to obtain the most negative Gibbs free energy for the system. Equilibrium conditions persist when the Gibbs free energy (ΔG) is at a minimum.

The PREDOM program calculates predominance diagrams. The concept of the predominance diagram was popularized by Kellogg and Basru²⁸ as an aid to visualizing the range of stabilities for metal-oxygen-sulphur systems. Since then, they have become an important tool for assessing the reaction conditions for many other systems. The authors of the F*A*C*T program have reviewed²⁹ the use and calculations of predominance diagram in detail, and proposed a new, efficient method for their calculation, and what particularly lends itself to the basis of a computational algorithm. A predominance diagram is a representation of all the compounds of a selected base element that are stable in relation to the partial pressures (activities) or ratios of other species.²⁴

APPENDIX III:

CALCULATION OF THE RATIO OF Al_2O_3 : C RATIO

The use of cane sugar and boehmite made it difficult to calculate the exact ratio of Al_2O_3 : C from the starting materials, due to the high water absorption rate of cane sugar, and the sedimentation of boehmite particles due to the pH changes resulting from the interactions between boehmite and water. To solve this problem, it was necessary to back calculate the Al_2O_3 : C ratios based on the weight changes after nitridation and decarburization. The amounts of converted AlN and residual carbon were calculated from the weight change after decarburization. The amount of Al_2O_3 was calculated from the amount of converted AlN, and the amount of carbon consumed, based on the stoichiometry of the nitridation reaction, was calculated. The total C was calculated by adding the consumed C and the residual C. The ratio of Al_2O_3 : C was then calculated from the total C and the amount of Al_2O_3 nitrided.

Below is an example of the above calculation: 1 mole of Al_2O_3 is 102 g, 1 mole of AlN is 41 g, 1 mole of C is 12 g, and 2 moles of AlN is produced from 1 mole of Al_2O_3 with 3 moles of C.

- (1) If 50 g of AlN was obtained from decarburizing 60 g of fully converted as-reacted product, 10 g of the as-reacted product was carbon.
- (2) The 50 g of AlN can be produced from 62.2 g of Al_2O_3 ($50 \text{ g} \times (82 / 102)$).
- (3) Assuming that the 62.2 g of Al_2O_3 was reacted with three times the amount of C, by molar ratio, the amount of C reacted was 22 g ($(62.2 / 102)$

x 3 x 12).

(4) The total amount of C in this precursor material can be assumed to be 32 g (10 + 22).

(5) Then the ratio of Al_2O_3 : C can be calculated as 1 : 4.4 (62.2 / 102 : 32 / 12).